ISSN 0010-9525, Cosmic Research, 2010, Vol. 48, No. 1, pp. 1–30. © Pleiades Publishing, Ltd., 2010.
Original Russian Text © Yu.I. Yermolaev, N.S. Nikolaeva, I.G. Lodkina, M.Yu. Yermolaev, 2010, published in Kosmicheskie Issledovaniya, 2010, Vol. 48, No. 1, pp. 3–32.

Relative Occurrence Rate and Geoeffectiveness of Large-Scale Types of the Solar Wind

Yu. I. Yermolaev, N. S. Nikolaeva, I. G. Lodkina, and M. Yu. Yermolaev

Space Research Institute, Russian Academy of Sciences, Profsoyuznaya st. 84/32, Moscow 117997, Russia

E-mail: yermol@iki.rssi.ru

Received November 11, 2008

Abstract—We investigate the relative occurrence rate for various types of the solar wind and their geoeffectiveness for magnetic storms with $D_{st} < -50$ nT. Both integrated effect for the entire time 1976–2000 and variations during this period of 2.5 cycles of solar activity are studied As raw data for the analysis we have used the catalog of large-scale types of the solar wind for the period 1976–2000 (see ftp://ftp.iki.rssi.ru/omni/) created by us with the use of the OMNI database (http://omni.web.gsgc.nasa.gov) [1] and described in detail in [2]. The average annual numbers of different type of events are as follows: 124 ± 81 for the heliospheric current sheet (HCS), 8 ± 6 for magnetic clouds (MC), 99 ± 38 for Ejecta, 46 ± 19 for Sheath before Ejecta, 6 ± 5 for Sheath before MC, and 63 ± 15 for CIR. The measurements that allowed one to determine a source in the solar wind were available only for 58% of moderate and strong magnetic storms (with index $D_{st} < -50$ nT) during the period 1976–2000. Magnetic clouds (MC) are shown to be the most geoeffective (~61%). The CIR events and Ejecta with Sheath region are three times less geoeffective (~20–21%). Variations of occurrence rate and geoeffectiveness of various types of the solar wind in the solar cycle are discussed.

DOI: 10.1134/S0010952510010016

1. INTRODUCTION

Solar wind formed as a result of expansion of the solar corona into the interplanetary space demonstrates a great variability at different temporal and spatial scales (see, for example, [3]). In this paper we, based on our catalog of large-scale solar wind phenomena [2], investigate mainly those variations with time scales from a few hours to 25 years which are closely related to dynamics of the solar atmosphere. These variations embrace 3 different intervals of characteristic times: (1) global variations of the Sun in the solar cycle (years), (2) scanning of large-scale and long-living solar structures due to rotation of the Sun with respect to a terrestrial observer (weeks), and (3) dynamic phenomena on the Sun and in the interplanetary space (days). In this case one should remember that an observer near the Earth's orbit has an opportunity to measure the solar wind only near the ecliptic plane, i.e., the solar wind originating at low heliolatitudes. Therefore, some global phenomena on the Sun in certain cases, taking into account geometry of the wind propagation, can weakly manifest themselves in solar wind streams. For example, the frequency of detection of the streams associated with coronal holes and CME can be not in correlation with the occurrence rate of coronal holes and CME on the Sun, if they are formed at high heliolatitudes. A detailed description of large-scale types of the solar wind and their connection with the Sun can be found in the proceedings of the "Solar Wind-11" conference held in 2005 [4] and in our paper [2], as well as in references therein. In Section 3 of the present paper we describe in detail the occurrence rate of different large-scale type of the solar wind on the scales of the solar cycle and period of rotation of the Sun.

The solar wind is the basic agent transferring energy from the Sun to the Earth's magnetosphere and producing magnetospheric disturbances. This property of various phenomena to be a source of magnetospheric disturbances is often referred to as geoeffectiveness. However, this term in modern literature is used in two senses: one should distinguish between geoeffectiveness of a certain type of the solar wind, i.e., the ratio of the number of events of a given type having resulted in a storm to the total number of events of this type, and effectiveness of the physical process of storm generation, i.e., the ratio of the output of this process (for example, the D_{st} index value) to its input (for example, a value of the B_z component of the interplanetarg magnetic field IMF or Akasofu parameter). Ignoring these distinctions one can arrive at incorrect conclusions. Only those types of the solar wind are geoeffective (in this paper, capable to generate magnetic storms) which include sufficiently large and prolonged southward ($B_z < 0$) component of the IMF [6–11]. Since in the steady-state solar wind the IMF lies in the ecliptic plane, the noticeable IMF component beyond the ecliptic plane can appear only in disturbed types of the solar wind. Magnetic clouds (MC) and compression regions before fast MC (Sheath) and on the boundary of interaction between fast and slow solar

wind streams (corotating interaction regions, CIR) represent such types of the solar wind (see review [12]).

Magnetic clouds are generated on the Sun as a result of coronal mass ejections in the form of a magnetic rope (a bunch of twisted magnetic field lines). Almost in all cases (excluding a rare case when the rope axis is directed northward) in one or another part the magnetic cloud contains the southward component of the IMF [13, 14]. There is recent trend to use in this area a slightly changed and complicated terminology: all manifestations of CME in the interplanetary space used to be called ICME (interplanetary coronal mass ejections) or Ejecta. Only a small part of them with strong and regularly rotating IMF are referred to as MC. The fraction of MC in the total number of ICME varies in the solar cycle [15]. The types Sheath and CIR are generated on the way from the Sun to the Earth as a result of interaction of a fast plasma volume (piston) with a slow plasma volume. ICME and fast streams from coronal holes serve as piston in the cases of Sheath and CIR, respectively. The IMF normal to the ecliptic plane originates due to compression and deformation of the region interacting streams (see, for example, [16]).

Numerous papers are dedicated to investigations into the role played by Ejecta/MC in generation of geomagnetic storms. For example, geoeffectiveness of Ejecta/MC (and of associated solar phenomena) is described in detail in reviews [17, 18], while geoeffectiveness of CIR is estimated in a single paper [19] using as example 727 events in the period 1964–2003, and it requires confirmation by independent investigations. Though in literature it was indicated more than once that Sheath could generate magnetic storms (see, for example, review [12] and references therein), the phenomenon of Sheath before MC/Ejecta became a subject of special in-depth studies rather recently (see [2, 20–26] and references therein). Moreover, in some papers [25–28] it was stated that during Sheath the process of storm generation turned out to be more effective than during magnetic cloud (without quantitative estimation of Sheath geoeffectiveness). Nevertheless, it should be noted that many researchers when studying a response of magnetosphere to various types of the solar wind do not distinguish between Sheath and MC/Ejecta [29–33]. In some papers authors do not take into account the fact that geoeffective types of the solar wind streams have much shorter duration than associated magnetic storms (for example, in recent paper [34] it has been demonstrated that durations of Sheath, MC, and CIR, generating magnetic storms with $D_{st} < -60$ nT, were equal in the period 1976–2000 to 9 ± 4 (for 22 events), 28 ± 12 (113), and 20 ± 8 (121) hours, respectively) and present the solar wind parameters for CIR, Sheath, and MC/Ejecta on intervals of 8–10 days [29, 35, 36]. In our opinion such an approach is incorrect and lead to wrong conclusions, since thus obtained results refer not to a given type of the solar wind stream, but rather to a mixture (usually, in unknown proportions) of several types.

It is also necessary to point out that there exist some additional fundamental unsolved issues which are connected mainly with methods and approaches in solving the problem.

1. Basically, only causes of the strong magnetic storms with $D_{st} < -100$ nT are investigated (see, for example, [23, 24]), i.e., the inverse correspondence (from a storm to its interplanetary source), rather than geoeffectiveness of various types of the solar wind, for which a list of interplanetary phenomena should be the original list of events, and one should search for them responses in the magnetosphere [37, 18].

2. Investigations of only strong magnetic storms (see the same papers [18, 23, 24, 37]) leads to a rather peculiar statistics of events: a small part of magnetic storms are investigated (those generated basically by interacting magnetic clouds [38, 6]), while less powerful storms, being more substantial in number, are not analyzed at all [39].

3. There is no analysis of the occurrence rate of all large-scale types of the solar wind over sufficiently long time intervals comparable with the solar cycle period.

4. No estimations of geoeffectiveness of Sheath are available in the literature.

We plan to overcome these drawbacks in the present paper. In our paper [2] we have described a catalog of large-scale types of the solar wind for the interval of 1976–2000 (see ftp://ftp.iki.rssi.ru/omni/) created using the OMNI database (http://omniweb.gsfc.nasa.gov) [1]. Therefore, we rest upon this catalog in this paper and investigate the relative occurrence rate of various types of the solar wind and their geoeffectiveness (for magnetic storms with $D_{st} < -50$ nT) both in general for the entire period under consideration and their variations in the solar cycle over the period 1976–2000 covering more than 2 solar cycles.

2. METHODOLOGY

Our catalog includes two parts: original parameters of the OMNI database supplemented by some derivative parameters calculated by us (for example, dynamic and thermal pressures, plasma beta-parameter, and some others), and the results of detailed (with a time resolution of 1 h) identification of 8 types of large-scale streams of solar wind plasma (HCS, Slow, Fast, CIR, Sheath, Ejecta, MC, and Rare), as well as two types of short-term events (interplanetary shocks IS and interplanetary reverse shock events ISA). A certain additional processing of data was accomplished to reach the purposes of this paper.

1. All phenomena of the Sheath type were divided in two subtypes: Sheath preceding Ejecta (Sh_E) and Sheath preceding MC (Sh_{MC}). This division is fully

determined by the criteria that have served as a basis for classifying Ejecta and magnetic clouds MC [2].

2. Annual numbers were calculated for the phenomena of all types and subtypes. Since duration of data gaps in the annual intervals can vary from 50% to 0%, it was necessary to reduce the obtained data to a unified scale. Such normalization was made under the assumption that the rate of appearance of a given type of stream is one and the same in the intervals with available data and in the data gaps. If in a selected year the number of detected events on the interval of data availability t_d was equal to N_e, then the normalized number of this type of phenomena in the given year was determined multiplying the rate of occurrence N_e/t_d for this type by the total year duration t_y. The numbers of events normalized in such a manner can be noninteger, their accuracy being the better the higher is the original values of N_e and t_d. One can estimate the error as $N_e^{-1/2}(t_y - t_d)/t_d$, i.e., at $N_e = 16$ and $t_d/t_y = 80\%$ the error is about 6%, and the normalized number of events in this example is approximately 20 ± 1. The error of a quantity expressed as a certain formula with simple quantities having known errors was determined as a square root of the sum of squared errors for all terms of the expression.

3. In order to determine geoeffectiveness we supplemented the archive with a list of magnetic storms with $D_{st} < -50$ nT. This list differs from a similar list used in previous papers (see, for example, [25–26]) in the following respect. In those papers we studied the time behavior of parameters for storms with $D_{st} < -60$ nT, since the D_{st} index very often behaves itself nonmonotonically during the storms in the range from –60 to –50 nT (multi-step magnetic storms), i.e., when one deals with sequences of magnetic storms (while one weak magnetic storm has no time to go through the entire cycle of its development, the development of the next storm begins). Cause-and-effect relations are strongly masked for such storms. The analysis has shown that the use of a bit stricter criterion $D_{st} < -60$ nT leads to a considerable reduction in the number of such complex storms. In this paper we returned to the classical definition of a storm in order that it could be possible to compare the obtained results (they basically include the number of events rather than the time behavior of parameters) with previous results for the storms with $D_{st} < -50$ nT.

4. Definite types of the solar wind streams were put in correspondence to all magnetic storms for which measurements of the parameters of plasma and magnetic field in the interplanetary medium were available. This was done using the following algorithm. If the moment of minimum in the D_{st} index from the list of magnetic storms falls within the time interval of a solar wind event or is apart from it by no more than 2 h interval (2 points), the corresponding solar wind type is ascribed to this storm. It should be noted that, according to the results of analysis of 64 intense ($D_{st} < -85$ nT) magnetic storms in the period 1997–2002, the average time delay between D_{st} peak and southward B_z component of the IMF is equal to ~2 h (see [40]). Similar results were obtained in papers [25, 34]. That is, two hours correspond to the average time delay between the D_{st} peak of an intense magnetic storm and the associated peak in the southward B_z component of the IMF.

5. When average durations of the types of solar wind streams were calculated, only those events were taken into account that neither began nor ended in the intervals of data gaps, i.e., whose duration was not distorted by the absence of data. The number of such intervals, naturally, can be lower than the total number of events. In this case, the standard deviation is presented as an error in the averaged quantity.

3. RESULTS

The general characteristic of the state of the Sun and magnetosphere in the time period under consideration, from 1976 to 2000, is presented in Fig. 1.

The left panel of Fig. 1 demonstrates variations of the solar activity (occurrence rate of strong X-ray flares of classes M and X), which is the main source of terrestrial disturbances. In order that the flares may be seen in the figure, their real duration was artificially increased up to 6 hours. The right panel of Fig. 1 shows the geomagnetic activity on the Earth corresponding to these flares (the occurrence rate of moderate $-100 < D_{st} < -50$ nT and strong $D_{st} < -100$ nT geomagnetic storms) during the time interval of 1976–2000 (left vertical axis) and according to the solar rotation number: Carrington rotations from 1636 to 1972 are given on the right vertical axis. This representation allows one to illustrate possible cause-and-effect connection between these phenomena observed in different space domains (solar flares on the Sun and magnetic storms on the Earth); one also can reveal and isolate long-living or repeating with the solar rotation (i.e., corotating) phenomena both on the Sun and on the Earth.

In the left panel one can see the variation of the annual distribution of X-ray flares of moderate (class M, gray intervals) and strong (class X, black intervals) intensity in the solar cycle: the largest numbers of X-ray flares are observed near the solar activity maximums of the 21st, 22nd, and 23rd cycles (clustering of points near the intervals of 1979–1982, 1989–1992, and 1999–2000, respectively). A similar behavior in the solar cycle demonstrates the geomagnetic activity (the value of D_{st} index), especially for strong magnetic storms with $D_{st} < -100$ nT (the right panel, black intervals). However, attempts to correlate separate events on the Sun and on the Earth fail in the majority of cases, which is indicative of a complex and ambiguous connection between the flares and storms [41]. In addition, it is well seen in the right panel that some magnetic disturbances (in particular, storms of moderate intensity represented by gray intervals) are

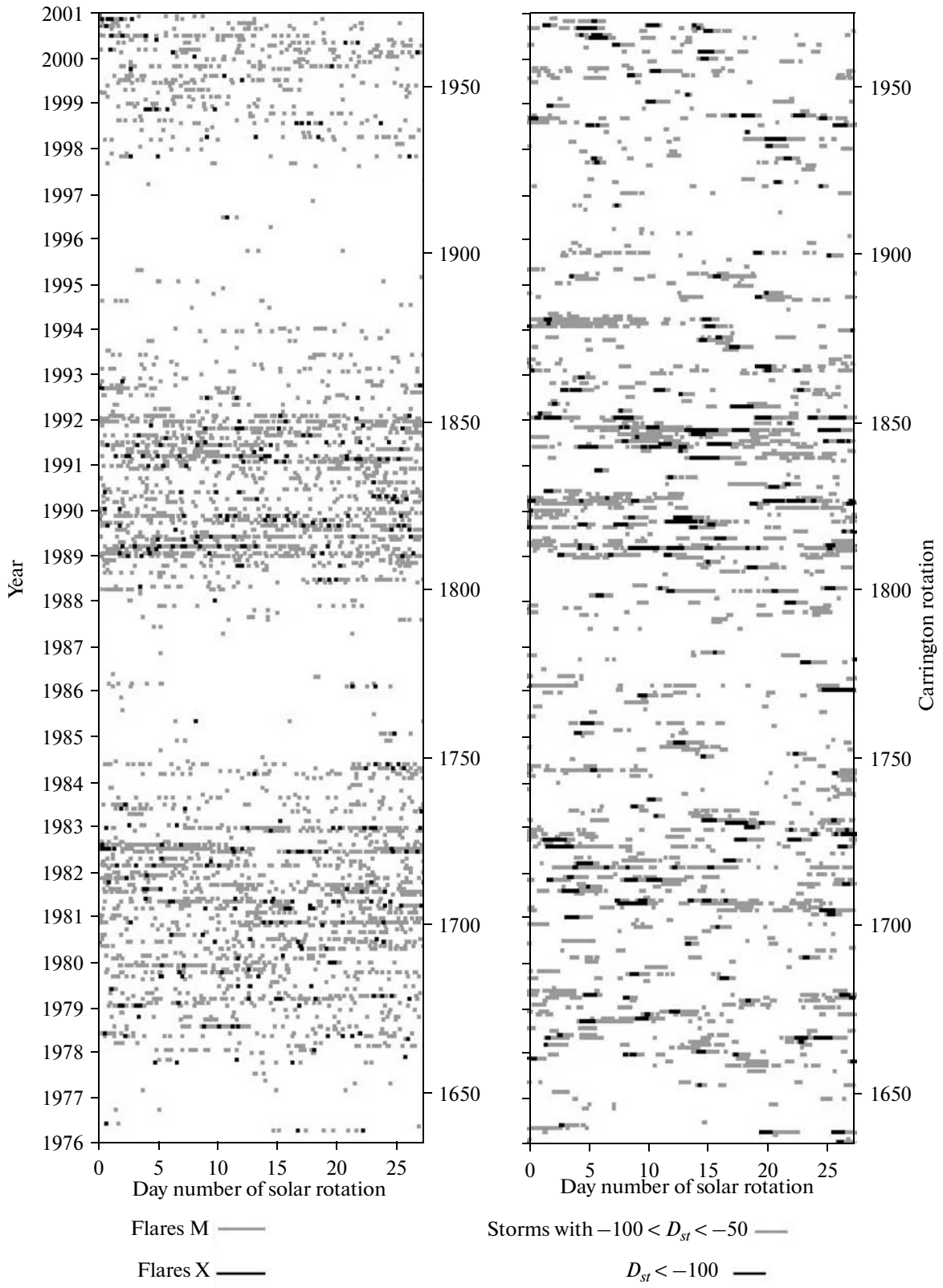

Fig. 1. The time of appearance of solar X-ray flares of classes M and X (left panel, gray and black intervals, respectively) and of geomagnetic disturbances of moderate and strong intensity (right panel, gray and black intervals, respectively) versus the day number of Carrington rotations of the Sun (horizontal axis).

repeated or exist for several sequential rotations of the Sun, i.e., they are possibly recurrent storms.

The solar wind is an agent transferring changes in the solar activity to the Earth, causing geomagnetic storms of differing intensities, as well as a variety of other phenomena both inside the magnetosphere and on the ground. Using the catalog of solar wind events and the list of moderate and strong magnetic storms in the period of 1976–2000 [2] we have performed a statistical analysis of the frequency of appearance of different types of the solar wind both over the entire time period and in accordance with phases of the solar cycle (Section 3.1). In addition, we have analyzed the duration distributions for each type of the solar wind, and have estimated the mean value of duration and variation of the mean annual duration with the solar cycle, as well as proportions between durations of different types of events (Section 3.2). We also investigated how for different types of events the geoeffectiveness changes in the solar cycle (Section 3.3).

3.1. occurrence rate of Large-Scale Events in the Solar Wind

The numbers of different types of the solar wind measured per year and their variation with changing solar activity in the period 1976–2000, or during 2.5 solar cycles (21st, 22nd, and a half of 23rd cycles) are presented in Fig. 2. The number of events of each type was estimated using the number of intervals of the given event type in a year. The events Fast and Slow presented in Fig. 2 belong only to the time intervals not associated with other events. The total number N of events of each type is indicated at every panel on the left. On the right the mean annual number of events of each type <*type*> is shown together with its root-mean square deviation. Although the number of events for separate years in Fig. 2 can be distorted due to gaps in measurements of the parameters of plasma and IMF, we present below some tendencies of their variation in the solar cycle. However, one should be careful with using these results, and further (Fig. 6) we return to this issue after normalization of the annual numbers of events.

As is seen in Fig. 2, events of the type Rare are indeed the type of events occurring least often: only 18 events over the entire period from 1976 to 2000. The events of this type are observed mainly near the sunspot maximums, a half of all events (9) being observed in the 21st cycle, 8 events were observed near the maximum of the 22nd cycle, and only 1 event in the beginning of the 23rd cycle of solar activity (see Fig. 2h).

Magnetic clouds MC are also not frequent events (101 MC events in total were observed for almost 2.5 cycles of solar activity), as well as subtype Sh_{MC} associated with them: only 79 MC events have regions Sheath (Figs. 2g and 2e). The largest numbers of MC events are observed on the phase of growth of the solar cycle. For example, the annual number of MC events is 2–4 events in the minimum of solar activity, while it reaches 12 and 15 on the growth phases of the 21 and 23 cycles of solar activity, respectively. However, during the 22nd cycle the number of MC events was pretty small, and the maximum number of MC events does not exceed 4 events per year.

The heliospheric current sheet HCS is the most frequent phenomenon: 1440 events for the entire period (Fig. 2b). The annual number of these events changes by an order of magnitude over several solar cycles, from ~10 (near the maximum of the 22 cycle) up to 220 events per year (near the minimum between the 22nd and 23rd cycles). One can conclude that the HCS events are more frequent near the sunspot number minimum.

The remaining types of streams occur with approximately equal frequency: there are from 18 to 42 events per year for CIR type (Fig. 2c), the number of Sh_E events (Shear regions of Ejecta) fluctuates from 8 near the minimum up to 40 events near the cycle maximum (Fig. 2d), the number of Sh_{MC} (Sheath regions of MC) is equal to 1–2 events near the minimum and increases to 8 to 11 events on the growth phase of the 21st and 23rd cycles (to 4 events on the declining phase of the 22nd cycle) (Fig. 2e), Ejecta events vary from 22–40 events near the minimum to 51–93 events near the maximum of solar activity (Fig. 2f). The types Fast and Slow give from 30 to 100 events per year and from 30 to 130 events per year, respectively (Figs. 2g and 2h). Though time variations of the numbers of different type of events are large (by a factor of 3–5), not all types of events, however, have variations synchronized with the solar cycle.

From 9 types of events presented in Fig. 2 only 5 types, namely, HCS, Sheath (both subtypes Sh_{MC} and Sh_E), Ejecta, and MC have well-pronounced dependence on the phase of solar activity or the sunspot number. At the same time for types CIR, Slow, and Fast the dependence on the solar cycle is weaker or absent.

Events of Ejecta and MC types prevail on the growth phase, including the cycle maximum. However, statistics of events is almost 10 times lower for MC in comparison with Ejecta, so that one can speak only about tendencies.

Events of the Sheath type that precede the Ejecta and MC events are characterized by a clear dependence on the solar cycle. First, they are rather frequent, about 48.1% of all Ejecta events have the Sheath region (543 Sh_E events out of 1128 Ejecta events). The fraction of Sh_{MC} events prior to magnetic clouds is even higher and reaches 78.2% (79 Sh_{MC} events out of 101 MC events). Second, the subtype Sh_{MC} is most frequently observed on the phases of growth and decline of the cycle, while subtype Sh_E is more frequent near the activity maximum. It is possible that the displacement of peaks of MC events having Sheath with respect to the peak of Ejecta with

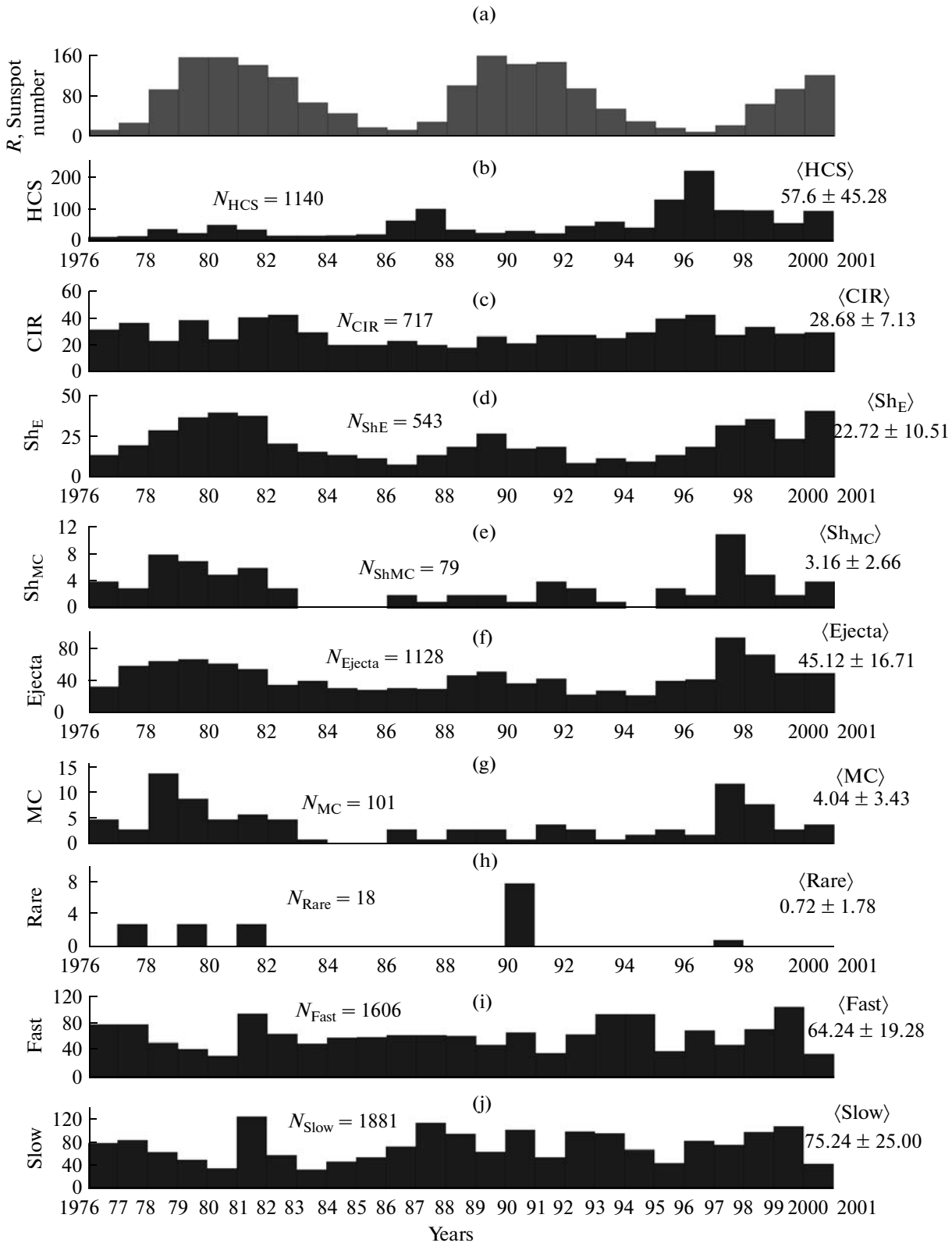

Fig. 2. Annual variations of year-averaged numbers of (a) sunspots and (b–i) different types of the solar wind.

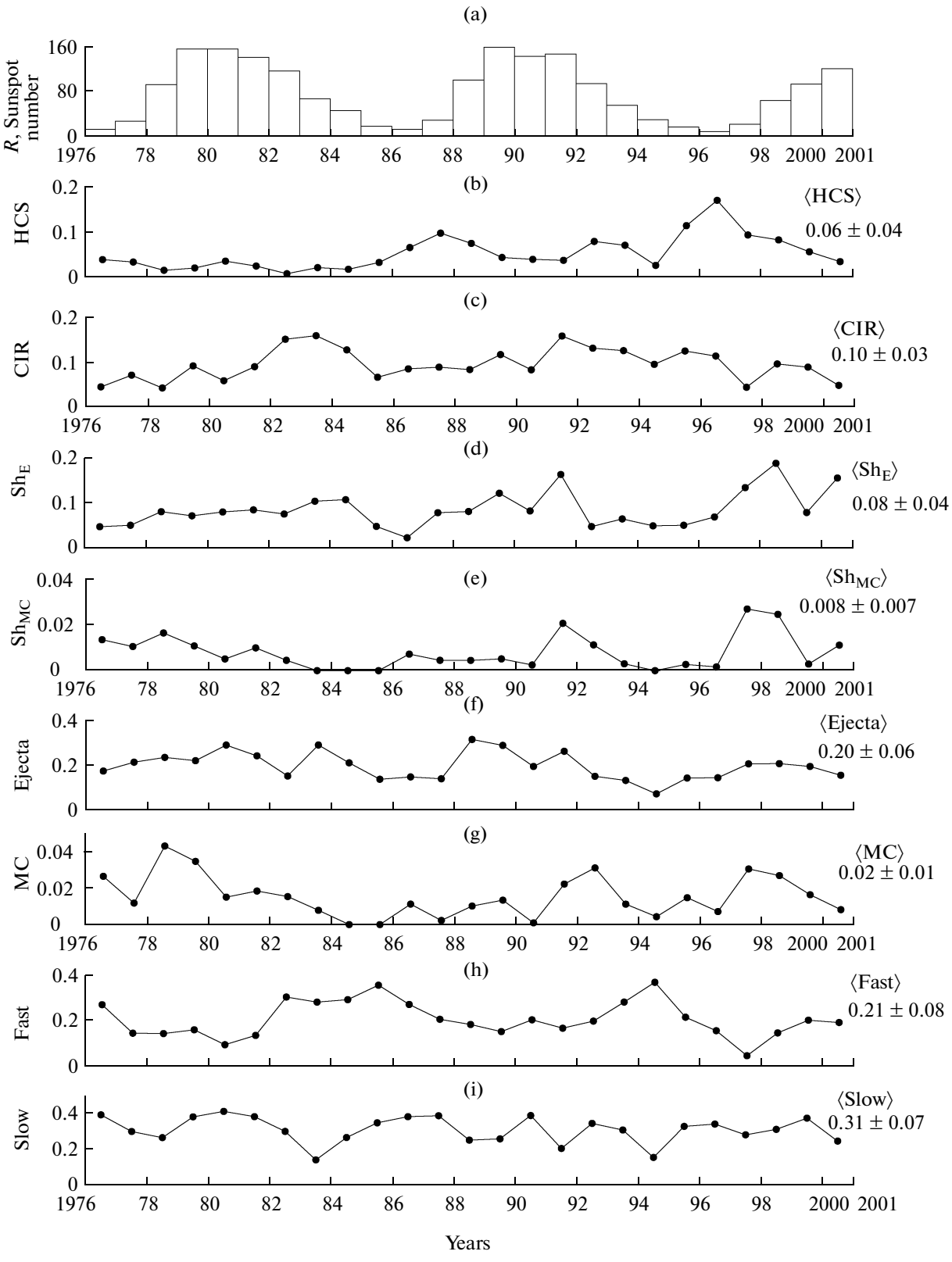

Fig. 3. The same as in Fig. 2 but for relative duration of observations of different types of the solar wind.

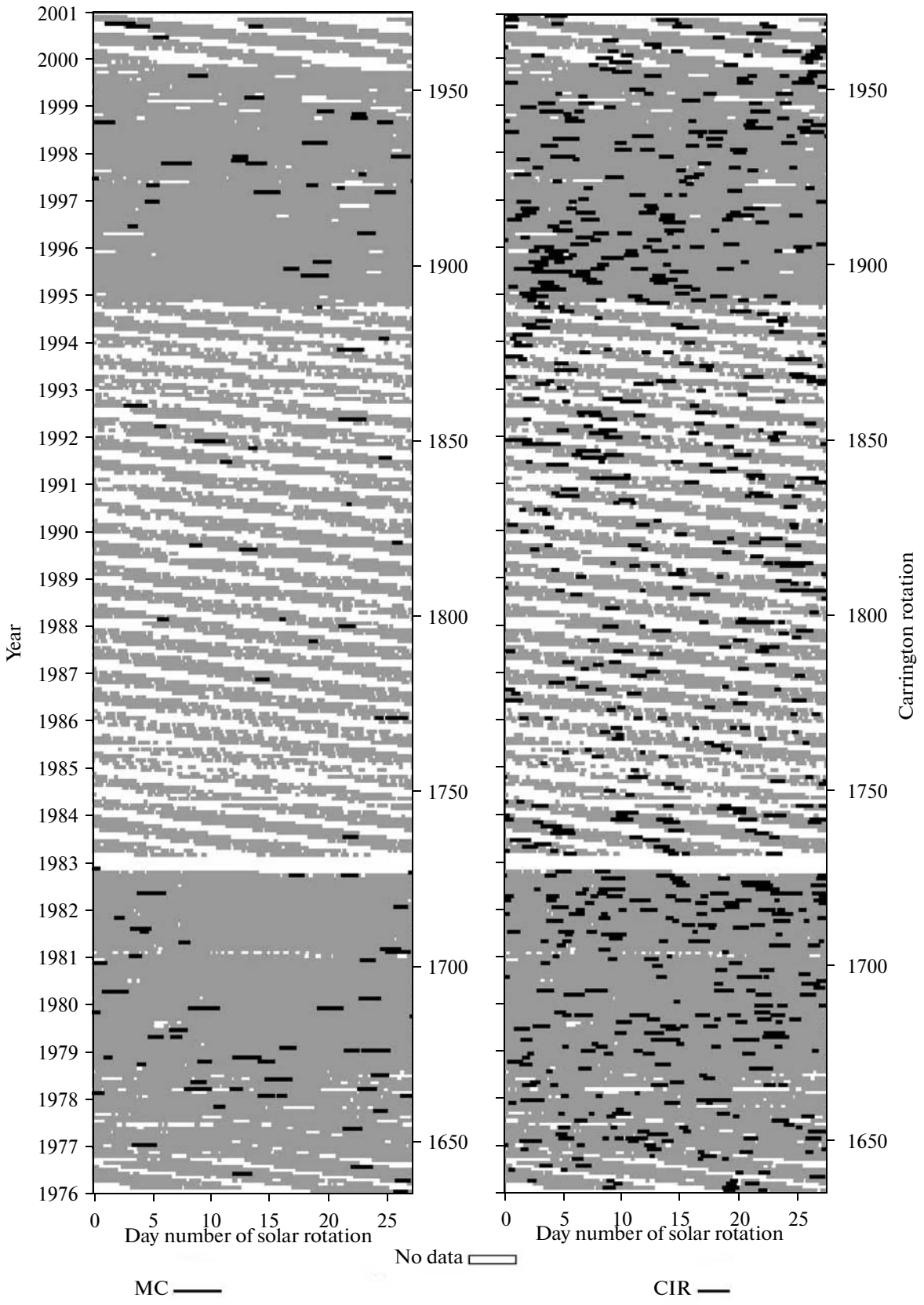

Fig. 4. The time of occurrence of events MC (left panel, black intervals) and CIR (right panel, black intervals) are presented as in Fig. 1. Gray color designates the periods when the data on plasma and magnetic field are available, the white color shows data gaps.

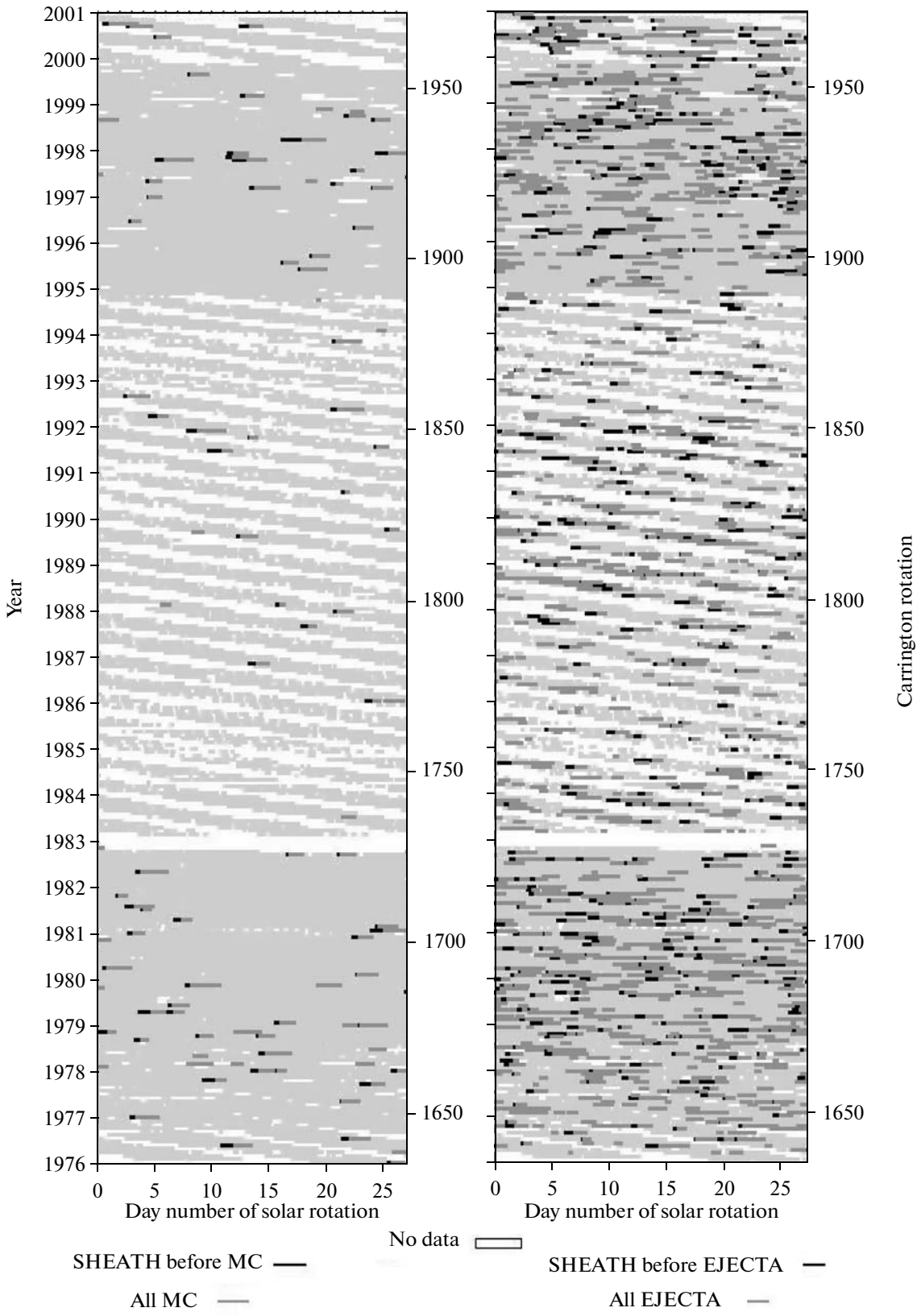

Fig. 5. The time of occurrence of events MC (left panel: all MC are shown by dark gray color, black intervals are Sheath before MC) and Ejecta (right panel: all Ejecta are shown by dark gray color, black intervals are Sheath before Ejecta) are presented as in Fig. 1. The light gray color designates the periods when the data on plasma and magnetic field are available, the white color shows data gaps.

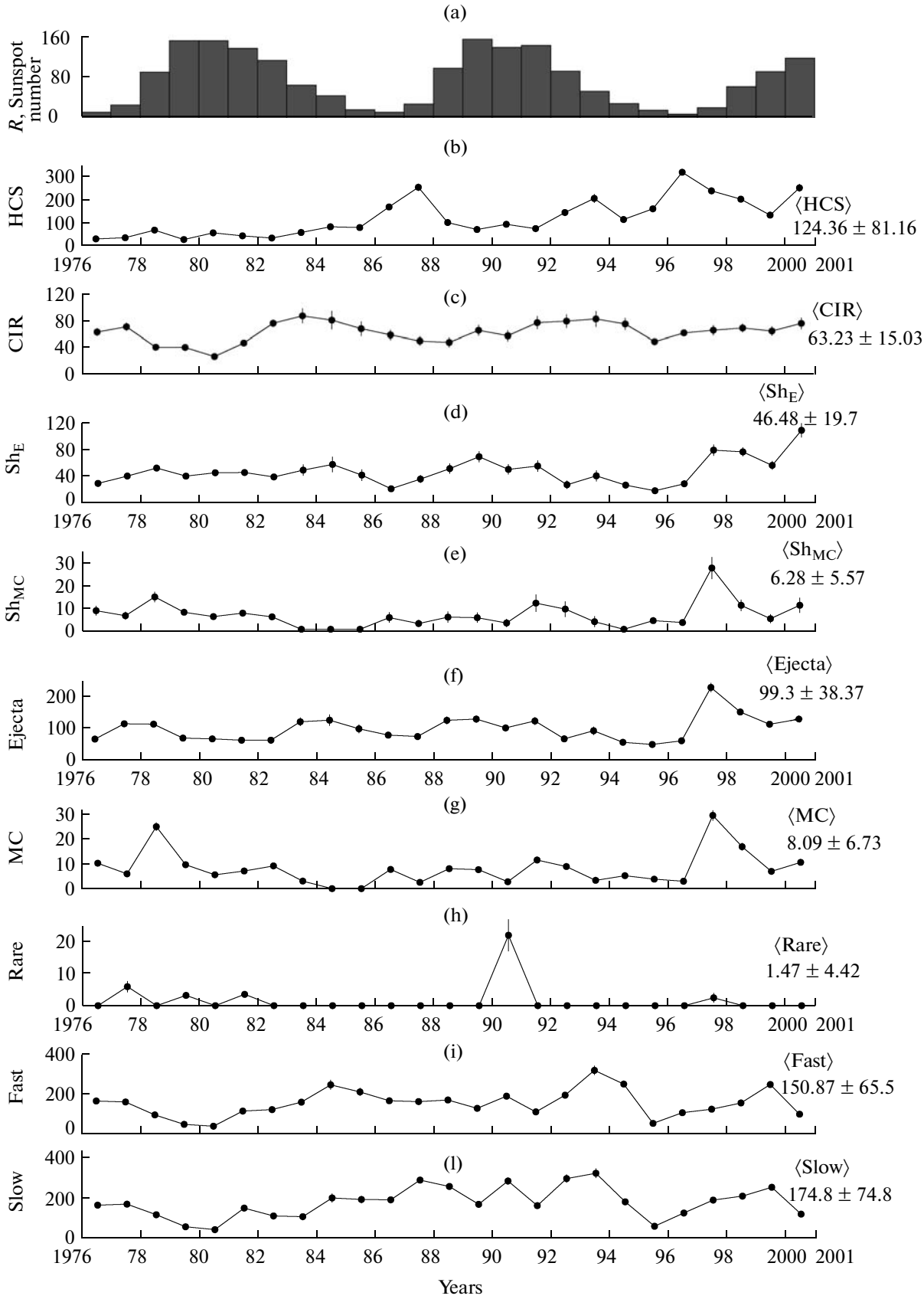

Fig. 6. The same as in Fig. 2, but with normalization (data gaps are taken into account).

Sheath is due to small statistics for MC events of this type.

The next Fig. 3 is similar to preceding Fig. 2, but instead of the number of intervals (events) of different solar wind types per year (as is the case for Fig. 2) it shows the mean annual fraction (in time) of each solar wind type, i.e., the ratio of observation time of a solar wind type to the total time of observation (total duration of intervals with measurements of plasma and magnetic field) in a year. Thus, the entire period of time from 1976 to 2000, when the plasma and magnetic field data were available, can be divided in different type of solar wind streams: approximately 6% of time the HCS type was observed, CIR events occupied ~10% of time, region Sheath before Ejecta was observed 8% of time, less than 1 % (~0.8%) of time falls on region Sheath before MC, about 20% of the total time is the share of Ejecta events, and ~2% of time falls on magnetic clouds MC. That is to say, the solar wind types mentioned above occupy only 47% of the total time for which the data on plasma and magnetic field were available. The remaining 53% of observation time cannot be identified with any of the solar wind types considered above. Out of this unidentifiable solar wind 21.5% falls on the fast solar with $V > 450$ km/s (the stream type Fast), and 31.5% of time is occupied by the slow solar wind (Slow type).

Some types of streams of the solar wind have a property of recurrence (for example, CIR events) with the rotation of the Sun, while other types of the solar wind streams are observed independently of the solar rotation. In order to reveal the recurrence of events or their periodicity with a solar rotation (~27 terrestrial days), we have taken advantage of the data representation similar to that of Fig. 1: information about events (their presence or absence) is set forth along the horizontal axis with days of Carrington rotations (from 1 to 27), while the numbers of Carrington rotations and years corresponding to them are laid off on the vertical axis.

Figure 4 presents the intervals of observations of MC events (left panel) and CIR events (right panel) as functions of the day of solar rotation (abscissa axis) in the period 1976–2000 (ordinate axis). Gray color demonstrates that data of the simultaneous measurements of parameters of plasma and magnetic field are available, while color designates the data gaps. CIR events recurrent with a period of 27 days manifest themselves as vertical clusters of black bars on the right panel. Such CIR events are especially well seen in the interval 1994–2000, when the number of data gaps is small. Also it is evident that not all out of CIR events identified by us are recurrent, and they may be observed on one rotation only. The number of corotating events CIR possessing the property of repeatability for two solar rotations and more is 100 (out of 717 CIR, i.e., 14%). Out of them, 72 CIR events are recorded during two successive rotations of the Sun (10% of the total number of CIR events), 15 CIR events (2% of all CIR events) exist for 3 rotations, 10 CIR events (1.4% of all CIR) live for 4 solar rotations, and only single CIR events survive during 5, 6, and even 10 successive solar rotations (3 events in total out of 717 CIR events, or 0.4%). Thus, only 14% (~20% with allowance made for data gaps) of all CIR events are recurrent, while 86% of all recorded CIR events (617 events out of 717), on the contrary, are not recurrent events, since they exist only during one rotation of the Sun.

Magnetic clouds MC appear any time, independent of each other (Fig. 4, left panel). However, one can see several MC events that were observed in two successive solar rotations, for example in 1981, 1982, 1998, 1999, and at the end of 2000. In total, 6 corotating MC events (out of 101 MC, ~6%) were found that were repeated during two successive rotations. The appearance of such repeating magnetic clouds MC is sufficiently rare event, and it needs further investigation.

In Fig. 5, similar to preceding Fig. 4, the intervals of observation are shown for all MC events and Sheath regions observed before MC (left panel), and all Ejecta with adjacent Sheath regions (right panel). We emphasize that regions Sheath adjoining the MC and Ejecta events are shown by the darkest color. It is interesting to note that the MC events in Fig. 4 suspected to be recurrent with the solar rotation have the Sheath region before the MC body.

On the other hand, Ejecta events shown in Fig. 5 (right panel) also can be recurrent and not only during 2–3 rotations (as it was the case for MC), but even during 5–7 rotations. And these recurrent Ejecta events can be without the Sheath region ahead them (see the right panel of Fig. 5, 1997, that is near the minimum of activity). At the same time, in 1980 the recurrent Ejecta events have Sheath regions (near the maximum of activity). Moreover, recurrent Ejecta events (both with Sheath and without it) are more numerous than recurrent events CIR. Partially this is explained by larger statistics of Ejecta events in comparison with CIR (717 CIR against 1128 Ejecta).

In order to take into account the data gaps in original data and to reduce the obtained results to a unified scale, a normalization procedure was used (see Section 2). Figure 6 presents the annual distribution of the amount of the same 9 types of the solar wind, but normalized to percentage of the time when identification of the types of streams is possible, i.e., when there are simultaneous data for the plasma and magnetic field. Vertical dashes show possible errors (uncertainty) for normalized number of events.

As a result of normalization, not only the total number of events of each type has changed, but for some types of events the variations of annual numbers have changed as well, which has had an impact on their behavior in the solar cycle. For example, upon normalization a tendency of solar-cycle dependence CIR type events has become better pronounced: more frequently CIR events appear on the phase of solar activity decline, near the minimum, but they became

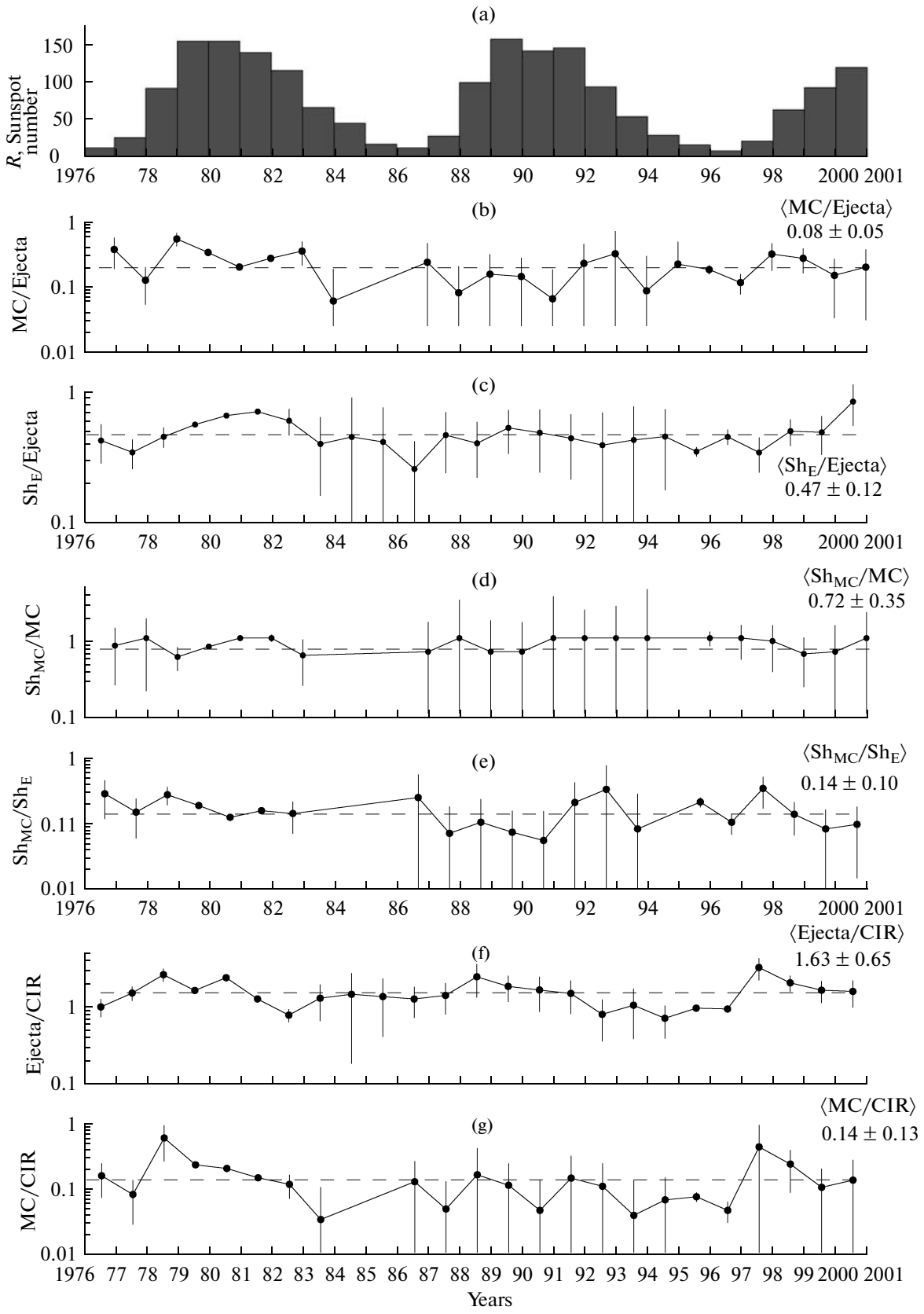

Fig. 7. Annual variations of (a) sunspot number and (b–g) the ratios of annual numbers for different types of the solar wind.

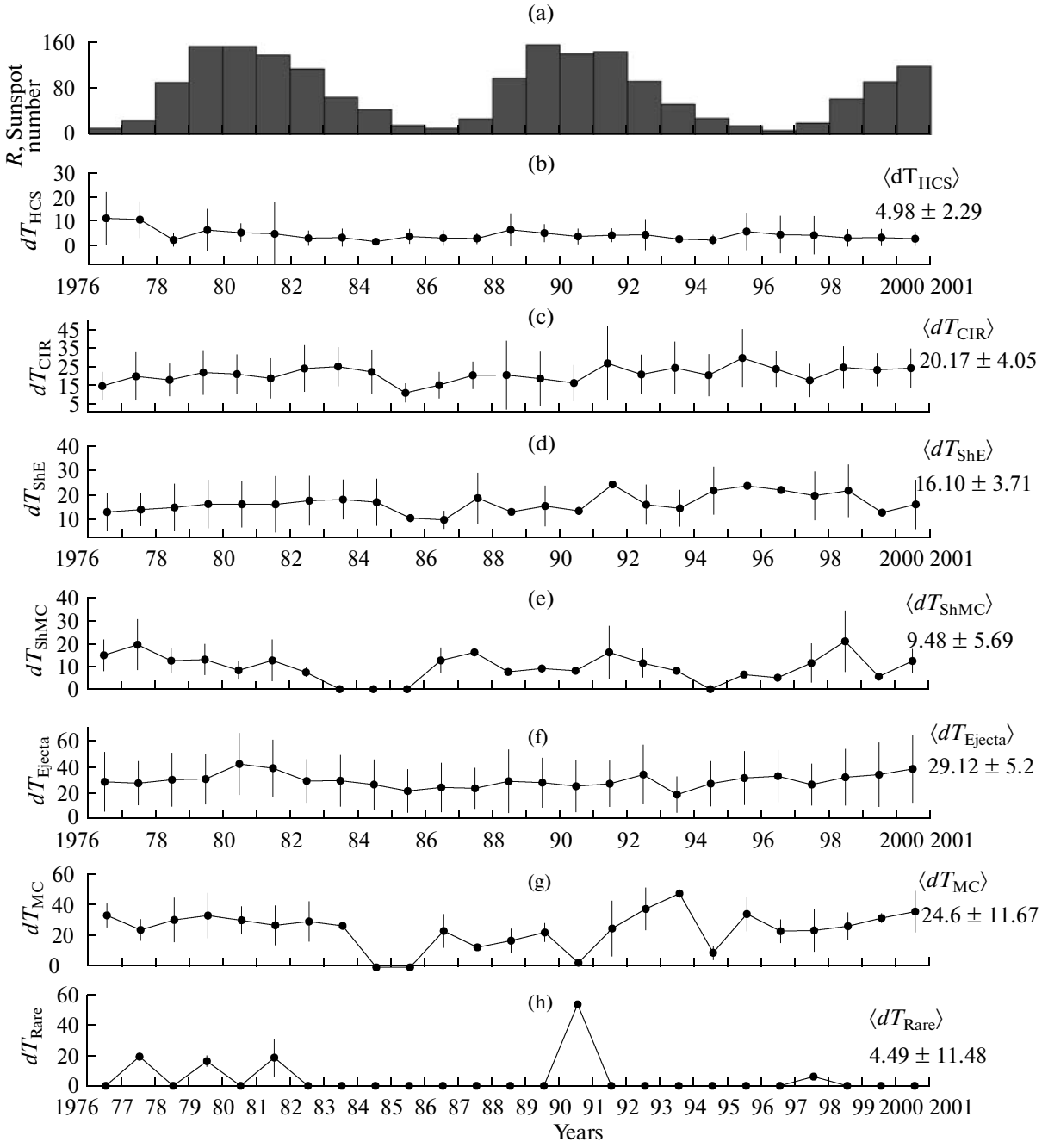

Fig. 8. Annual variations of year-averaged (a) sunspot numbers and (b–h) durations of different types of the solar wind.

less frequent near the maximum of solar activity (Fig. 6c). Before the normalization, this tendency revealed itself only slightly. However, a large uncertainty allows one to speak only about tendency of this dependence.

At the same time, Sheath events (both subtypes Sh_E and Sh_{MC}) after the normalization demonstrate weaker dependence on the solar cycle than before normalization (Figs. 6d and 6e). The predominance of these events near the growth phase (for Sh_{MC}) and solar activity maximum (Sh_E) remains, but this tendency is very weak and less pronounced than for events without normalization. Let us remind that statistics of Sh_{MC} events is small (less than for Sh_E by a factor of ~7), while errors are large and comparable in magnitude with the mean annual value.

One can suppose that the normalized numbers of Ejecta events including all subtypes have two maxima

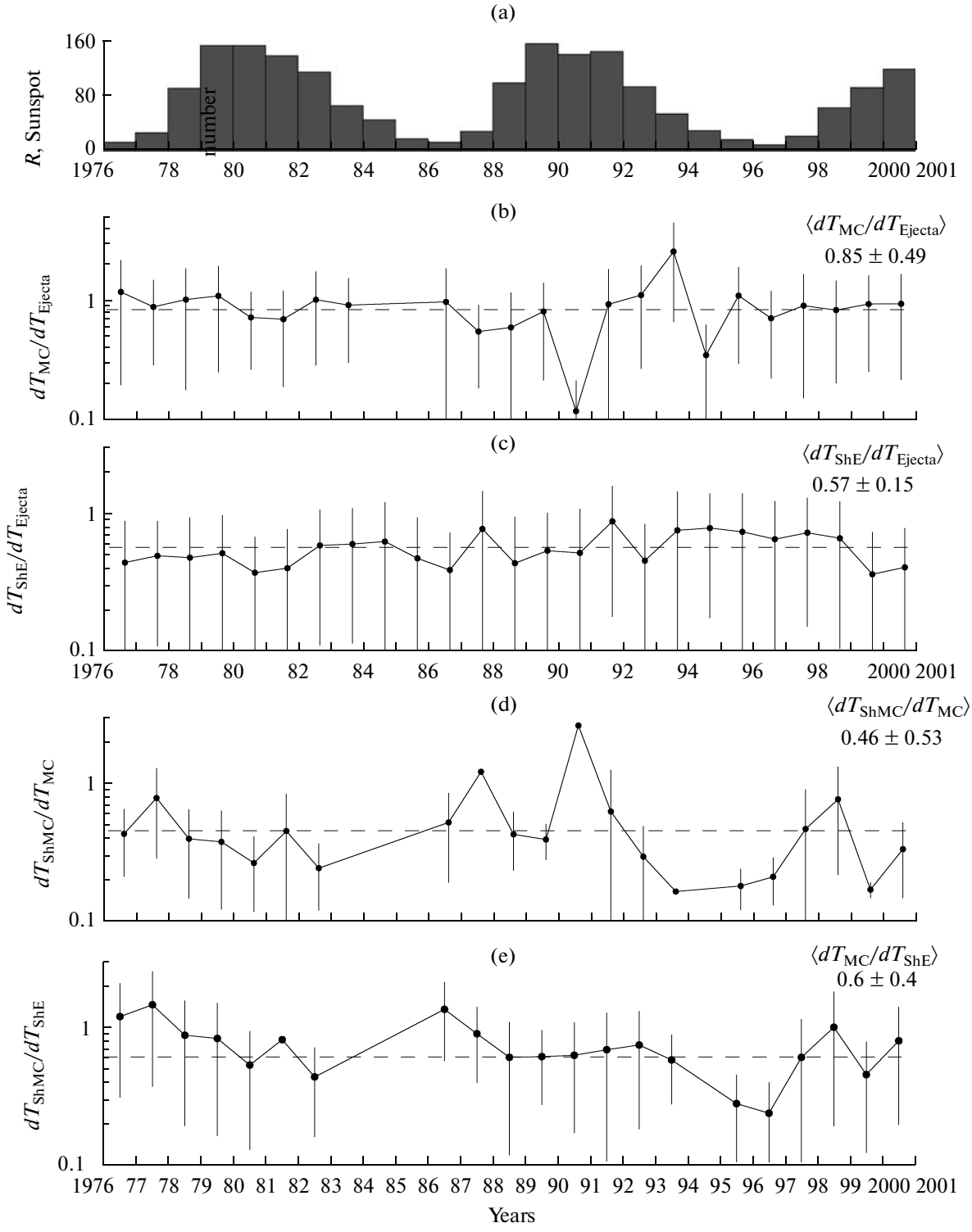

Fig. 9. Annual variations of (a) sunspot numbers and (b–e) the ratios of durations of different types of the solar wind.

in each cycle (Fig. 6f): the number of events increases on the phases of growth and decline of solar activity. At the same time, for normalized MC events the peaks are observed in the beginning of the growth phase of solar activity (Fig. 6g). One can also suppose that after the normalization a tendency of prevalence of the slow streams near the maximum and of fast streams near the minimum of solar activity has made itself clearly seen.

The next Fig. 7 presents in logarithmic scale the variation of ratios of normalized annual numbers of various types and subtypes of events: (b) all events

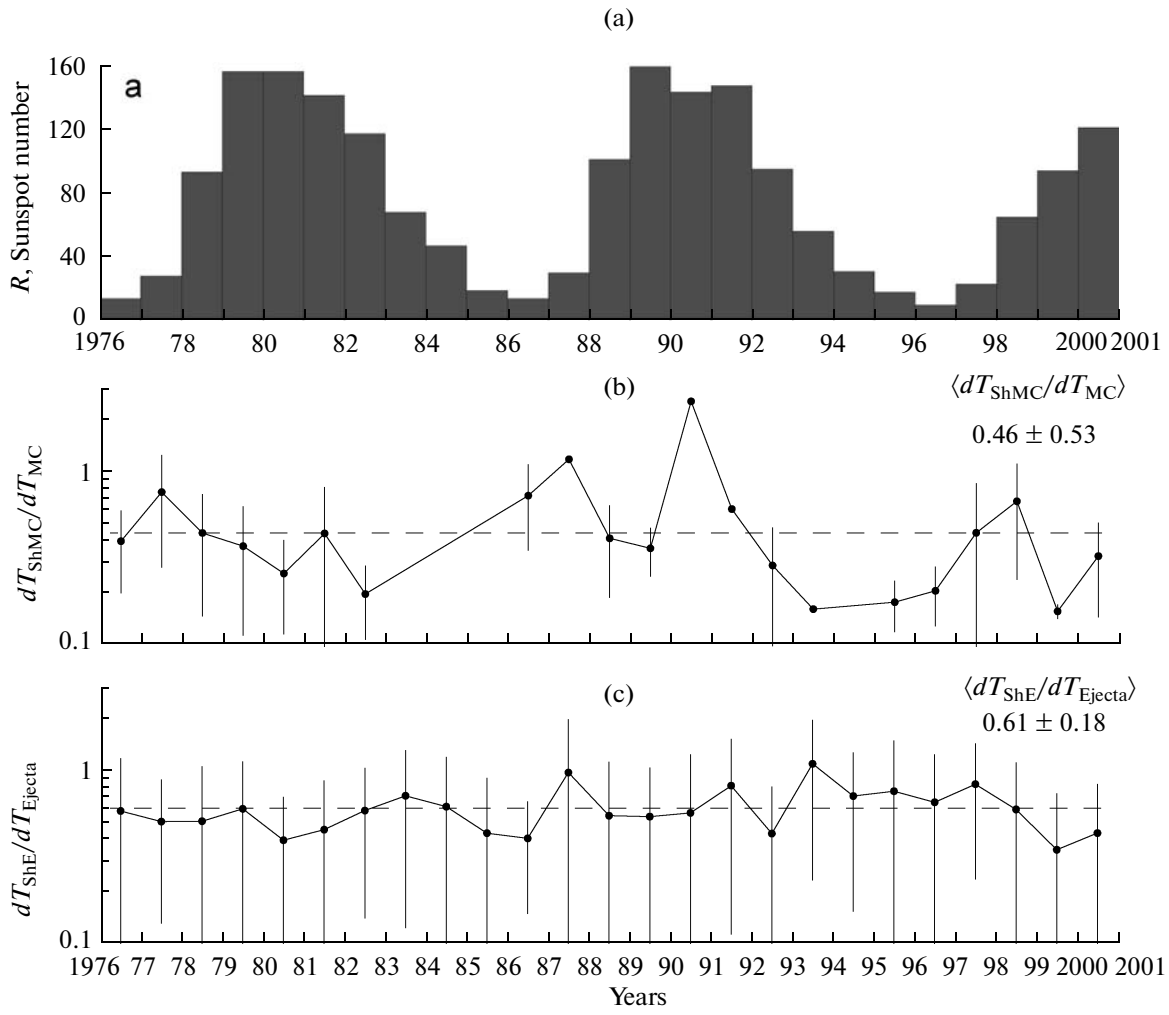

Fig. 10. Annual variations of (a) yearly sunspot numbers, and of the ratios of mean yearly durations of adjoining regions Sheath to their MC and Ejecta events: (b) dT_{ShMC}/dT_{MC} and (c) dT_{ShE}/dT_{E}.

(MC/Ejecta), (c) subtype Ejecta with Sheath to all Ejecta (Sh_E/Ejecta), (d) subtype MC with Sheath to all MC (Sh_{MC}/MC), (e) subtypes MC and Ejecta with Sheath (Sh_{MC}/Sh_E), (f) Ejecta type to CIR events (Ejecta/CIR), and (g) MC events to CIR events (MC/CIR). Figure 7a presents the variation of annual sunspot numbers. Each panel (b–g) presents on the right the annual ratios, averaged over the entire period from 1976 to 2000 (also shown by dashed lines), and their scatter (standard deviations). Vertical bars in Fig. 7 show possible errors in the ratios of event numbers (see Section 2).

One can see in Fig. 7b that MC events are observed substantially less frequently than Ejecta events. Throughout the entire period of time the mean annual number of MC events with respect to Ejecta events is equal to about 8% (with a scatter of 5%). During this time the annual fraction of MC events with respect to Ejecta events varies by a factor of 4 ranging from 5% to 22%. However, it should be noted that due to a large scatter (whose value is comparable with the value of the ratio itself) one can only suppose the following tendency. The frequency of MC occurrence (with respect to Ejecta) has two peaks: it increases near decline and growth of solar activity (where it is equal to 10–22%) but decreases by a factor of ~4 near the minimum and maximum of solar activity (down to 2–9%). That is, on the phases of decline and growth of solar cycle the fraction of MC with respect to Ejecta is twice higher than at minimum and maximum of the solar cycle.

How frequent are the regions Sheath before Ejecta events is illustrated by Fig. 7c. One can see that all the time the fraction of Sheath events of Ejecta, Sh_E, varies relative to the total number of Ejecta events by a factor more than 3, between 25% and 85% (Fig. 7c). On the average, in the entire period about a half of all Ejecta events had the Sheath region, $\langle Sh_E/\text{Ejecta}\rangle \sim 0.47 \pm 0.12$ (see Fig. 7c). However, possible errors in the annual ratios are very large, especially in the 22nd cycle,

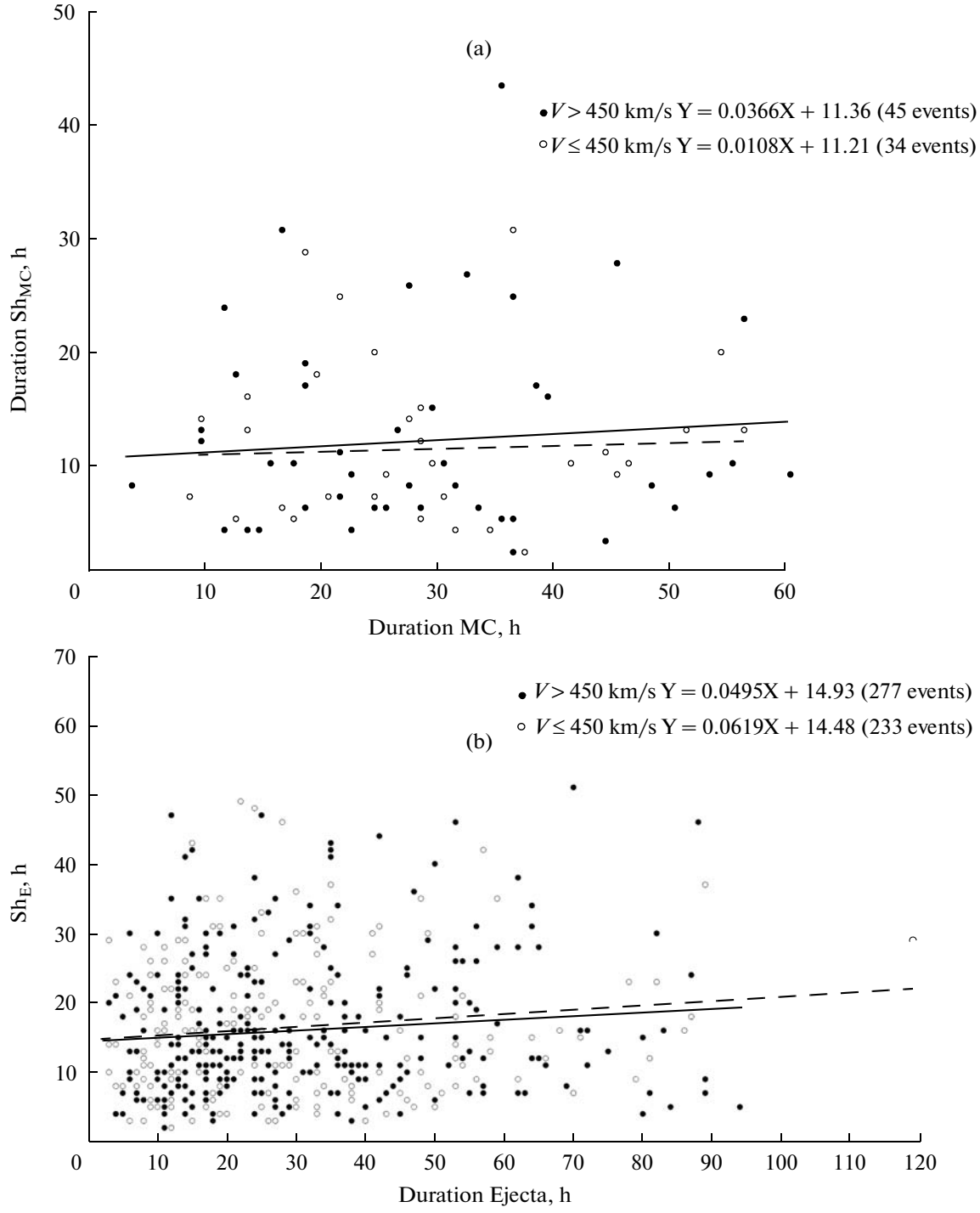

Fig. 11. Dependences of (a) duration dT_{ShE} on duration dT_{Ejecta} and (b) duration dT_{ShMC} on duration $dT_{MC,}$ respectively, for Ejecta and MC moving with velocities $V < 450$ km/s (light circles, approximation by the dashed line) and $V > 450$ km/s (black circles, approximation by the solid line).

because of long intervals with data gaps. One can suppose that there is a tendency of increasing number of Ejects events having the region Sheath near the solar activity maximum. For example, for the 21st cycle the ratio changes from ~35% immediately after the minimum up to ~80% immediately after the maximum. A weaker dependence is observed for the 22nd cycle (from 30% at the minimum to 50% at the maximum), but possible errors here are especially large (see vertical bars in Fig. 7c). It is possible that for the 23rd cycle the fraction of Ejecta with Sheath increases from 40% near the minimum up to 90% near the sunspot maxi-

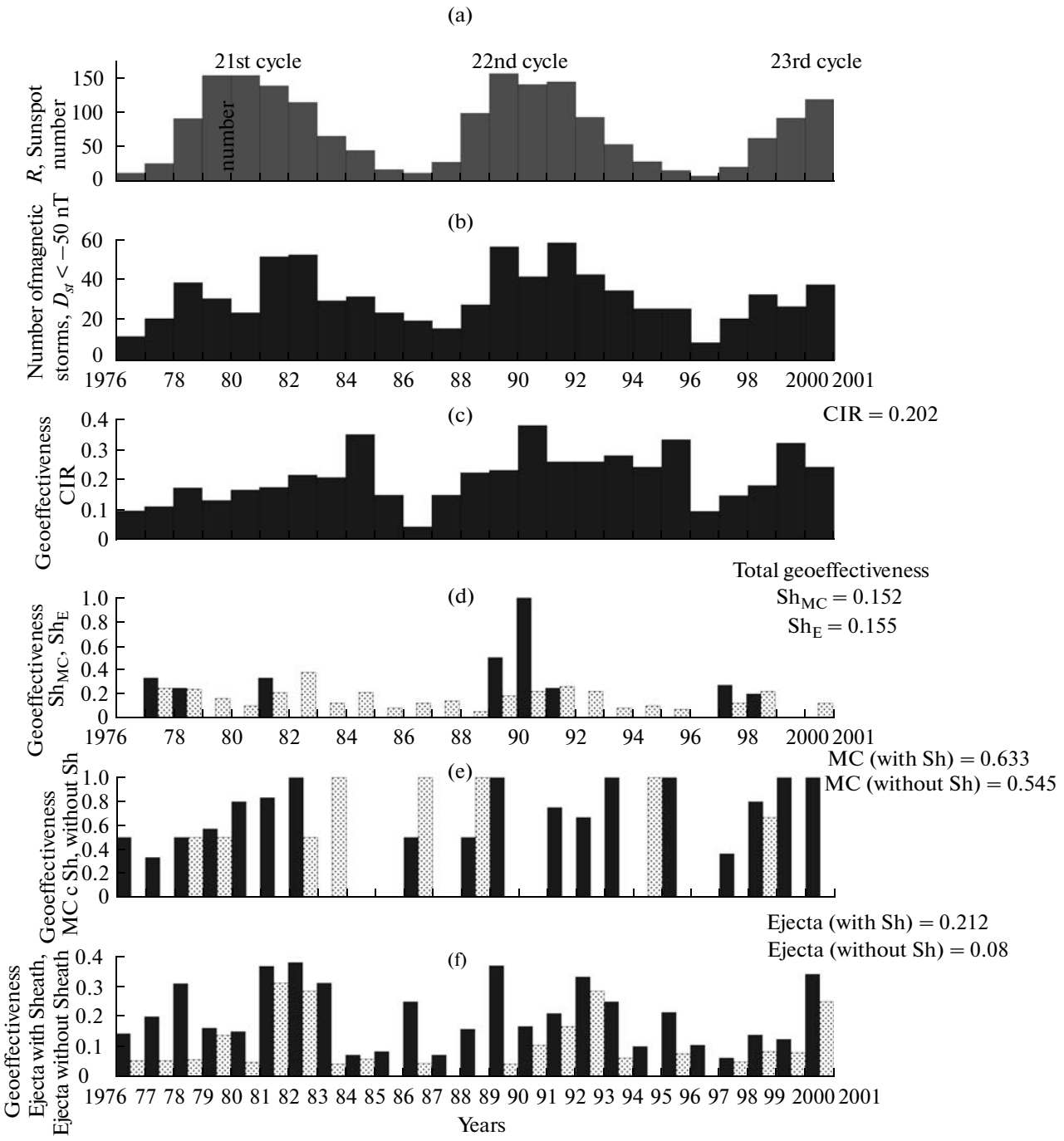

Fig. 12. Annual variations of (a) sunspot number, (b) magnetic storms, and (c–f) geoeffectiveness for different types of the solar wind.

mum. Thus, one can assume that Ejecta events with Sheath region occur twice more frequently near the maximum of the solar cycle.

Figure 7d presents the fraction of MC events with Sheath region with respect to all events of MC type. The all-time averaged value of this ratio is $\langle Sh_{MC}/MC \rangle = 0.72 \pm 0.35$, i.e., about 70% (though with large scatter) of MC events had a Sheath region. The frequency of appearance of MC events having a Sheath region varies between 55% and 100% over the entire time period. Very often, for example in 1990–1993 the fraction of Sheath events is 100% in MC type, that is all MC events have the Sheath region. The maximum fraction (up to 100%) of Sheath before MC events is observed on the phases of growth and decline of solar activity, while near the minimum of activity the fraction of MC

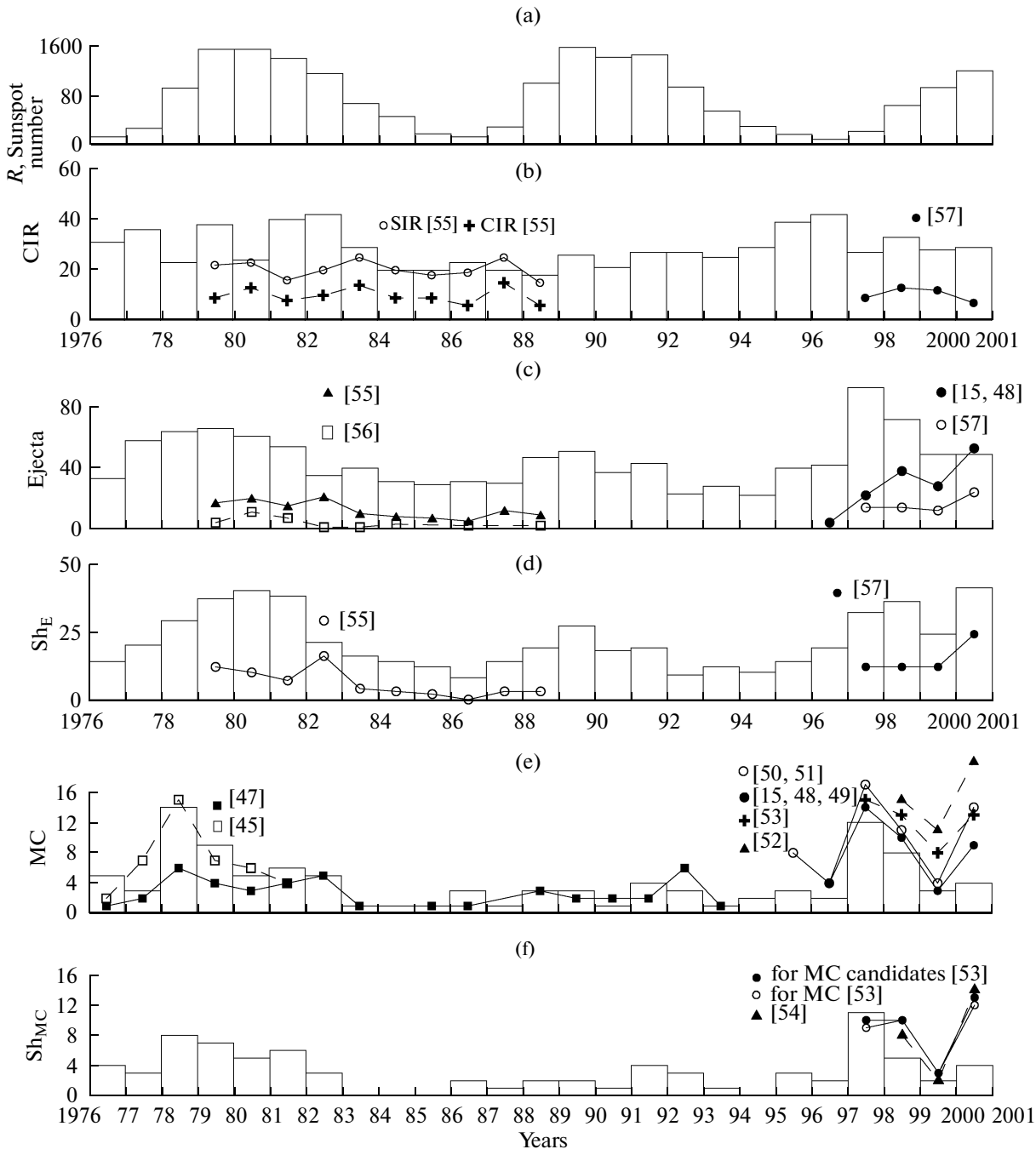

Fig. 13. Variations of the yearly numbers of (a) sunspots, and (b–f) different types of the solar wind according to our data (histograms) and the data of [15, 45, 47–57] (points and lines).

events with Sheath decrease down to 55–65%. However, possible errors in the ratios are very large, statistics of MC events is small, and one can only suggest a tendency of bifurcation for the peak near the maximum (i.e., the occurrence rate of Sheath events probably has two peaks both for MC and Ejecta: on the ascending and descending parts of the solar cycle).

Figure 7e shows the variation of the ratio Sh_{MC}/Sh_E of the numbers of Sheath events for MC and Ejecta types. The mean annual ratio averaged over the entire time interval is $\langle Sh_{MC}/Sh_E \rangle \sim 0.14 \pm 0.1$, i.e., the mean annual fraction of Sheath events for MC is approximately 14% with respect to Sheath events adjoining Ejecta. Over three solar cycles the ratio of these types of events is variable in a wide range between 8% and

35%, that is, more than four times. The number of Sheath events adjoining Ejecta substantially exceeds the number of Sheath adjoining MC by a factor of 3 as a minimum and reaches a factor of 12. However, because of a large scatter of the ratios no dependence on the solar cycle is seen. The larger statistics of events is required.

Figure 7f shows how the ratio of the numbers of events Ejecta and CIR (Ejecta/CIR) varies from year to year. The annual ratio averaged over the entire period 1976–2000 is $\langle \text{Ejecta/CIR} \rangle = 1.63 \pm 0.5$, i.e., the number of Ejecta events exceeds the number of CIR events by a factor of more than one and a half. Because of large scatter one can only suppose that the ratio Ejecta/CIR depends on the solar cycle: it is maximal and exceeds the mean ratio (Ejecta/CIR > 1.63) on the phase of growth of the solar activity, and it is minimal and lower than the mean ratio (Ejecta/CIR < 1.63) on the declining phase of solar activity, including its minimum.

Figure 7g illustrates the ratio between annual numbers of MC and CIR events. When averaging over the entire time interval, the ratio is $\langle \text{MC/CIR} \rangle = 0.14 \pm 0.13$, i.e., on the average the number of MC events is only 14% of CIR events. However, the variation with the solar cycle is seen, and the ratio MC/CIR changes from 0.03 to 0.8 with a maximum on the growth phase of the solar cycle (especially for the 21st and 23rd cycles) and a minimum on the declining phase (of the 21st and 22nd cycles). However, a large scatter in the ratio MC/CIR whose value is comparable with the value of the ratio itself does not allow one to make a final conclusion. One can only speak about tendencies in variations. Additional investigations are required.

3.2. Distributions of Event Duration for Different Types of the Solar Wind

The distribution of year-averaged duration dT (in hours) of different types of the solar wind is shown in Fig. 8. The values of duration averaged over the total period from 1976 to 2000 are presented on the right with their root mean square deviations.

The mean duration is the least for HCS events: $\langle dT_{HCS} \rangle = 4.98 \pm 2.29$ h. The longest duration is observed for events Ejecta, MC, and CIR, it equals tens of hours and even days: $\langle dT_E \rangle = 29.12 \pm 5.20$ h, $\langle dT_{MC} \rangle = 24.6 \pm 11.67$ h, and $\langle dT_{CIR} \rangle = 20.17 \pm 4.05$ h, respectively. The mean duration of events MC and CIR is approximately identical (~1 day). At the same time the mean duration of Sheath of MC events ($\langle dT_{ShMC} \rangle = 9.48 \pm 5.69$ h) is almost 1.5 times shorter than that of Ejecta ($\langle dT_{ShE} \rangle = 16.10 \pm 3.71$ h).

One can see in Figs. 8d and 8e that during 2.5 cycles of solar activity the mean annual duration of Sheath for MC events changes by a factor of 4 (dT_{ShMC} from 5 to 20 h) and duration of Ejecta Sheath varies twice (dT_{ShE} from 20 to 40 h).

With changing phase of solar activity the HCS duration varies between 3 and 12 h, i.e., by a factor of 4, with a peak near the minimum and beginning of the growth phase of the solar cycle. However, the scatter in duration of different types of events is large and often comparable with the value of this duration (see vertical bars in Fig. 8b). Similar situations are observed for all types of events presented in Figs. 8b–8h. One can assume that due to a large scatter the durations of all considered events do not depend on the solar cycle (or this dependence is weak).

The variation of the ratio of durations for different types of events and their subtypes is presented in Fig. 9 in the logarithmic scale. Dashed line in each panel shows the duration ratio derived from annual averaging over the entire period (numbers on the right in panels).

Figure 9b shows the ratio between year duration of MC and Ejecta events (including all subtypes) in the period of 21st – 23rd solar cycles. It is seen that on the average the duration of MC events is close to that of Ejecta, the average ratio $\langle dT_{MC}/dT_{Ejecta} \rangle = 0.85 \pm 0.49$, i.e., the mean duration of MC is 85% of Ejecta duration, but with a large scatter (49%). Throughout the full period the ratio of the annual duration of MC to the annual duration of Ejecta events varies between 0.5 (a single MC event was in 1990) and 1.3, only in 1993 it is equal to 2.5 (a single MC event was observed in 1993). Taking large scatter into account, one can suppose that the duration of MC events almost coincides with the duration of Ejecta events (shorter by 15%) and does not vary with the solar cycle.

Figure 9c demonstrates how the duration of Ejecta Sheath correlates with the duration of Ejecta events proper (with all subtypes). The mean duration of Sheath is always smaller than the duration of Ejecta events (twice on average, since the duration ratio is $\langle dT_{ShE}/dT_{Ejecta} \rangle \sim 0.57 \pm 0.15$). In the activity cycle the ratio between duration of Sheath and Ejecta varies by a factor of 2, from 0.4 to 0.8. However, because of large scatter there is no dependence on the solar cycle, or it is very weak.

Figure 9d shows the variation of the ratio between durations of MC Sheath and MC (all types). It is seen that for MC events duration of Sheath is also considerably shorter than duration of MC, excluding the years 1987 (only one MC event occurred in 1987) and 1991 (four MC events and all with Sheath regions), when the Sheath duration exceeded the MC duration by factors of 1.2 and 2.5, respectively. However, on the average for the entire time period the duration ratio is $\langle dT_{ShMC}/dT_{MC} \rangle = 0.46 \pm 0.53$, i.e., the Sheath duration is approximately twice shorter than the MC duration, but with a large scatter, close to the duration ratio value itself. Because of small statistics of MC events, strongly scattered values of MC duration and large errors in duration ratios of Sheath regions and MC, it is difficult to discuss any dependence of the duration ratio on the solar cycle phase.

Figure 9e presents the ratio between annual durations of Sheath regions before MC and before Ejecta events (dT_{ShMC}/dT_{ShE}). On the average, the annual duration of Sheath of MC events is approximately a half of the duration of Sheath before Ejecta ($\langle dT_{ShMC}/dT_{ShE}\rangle = 0.6 \pm 0.4$), but with a large root mean square deviation. In different years the ratio between durations of Sheath of MC and Ejecta events can vary strongly: from a very high value $dT_{ShMC}/dT_{ShE} = 1.5$ (in 1977) to a very low $dT_{ShMC}/dT_{ShE} = 0.25$ (in 1996). However, because of a large scatter, comparable with the ratio value, one can suppose that there is no dependence on the solar cycle, or it is very weak.

The next Fig. 10 presents the ratios of mean annual durations of Sheath adjoining in time to MC events (Fig. 10b) and Ejecta events (Fig. 10c), i.e., only for subclasses Ejecta with Sheath and MC with Sheath. The duration ratios in Fig. 10 were estimated using the ratio of durations averaged over a year. One can see in Fig. 10b the Sheath duration is on average shorter than that of adjoining MC almost twice (see the duration ratio over the entire period on the right). In the course of time the Sheath duration can vary within wide limits: from 0.1 up to 0.8 of the duration of adjoining MC, with exceptions in 1987 and 1990, when the Sheath duration exceeded the duration of MC adjoining it by factors of 1.2 and 2.7, respectively. The scatter of duration ratios is extremely large, therefore, there is no dependence on the solar cycle phase, or it is very small. Notice that the data presented in Fig. 10b (for ratios of Sheath duration to the duration of adjoining MC) do not almost differ from those of Fig. 9d (the ratio of Sheath duration to the duration of all MC). Though the statistics is different for MC events and subtype MC with Sheath (101 events and 79 events, respectively), this had no significant effect on the time behavior of annual ratios.

As it is seen in Fig. 10c, the Sheath duration is also shorter than that of adjoining Ejecta, excluding 1987 and 1993, when the duration ratio was close to unity (about 0.95 and 1.1, respectively). On the average, the Sheath duration is slightly higher than a half of the Ejecta duration ($\langle dT_{ShE}\rangle/\langle dT_{Ejecta}\rangle = 0.61 \pm 0.18$). In the course of time the Sheath duration varied from 0.4 and 1.1 of the duration of adjoining Ejecta. Taking large scatter into account, one can assume that the ratio of Sheath duration to the duration of adjoining events is practically identical for MC and Ejecta events, and it does not depend on the solar cycle or this dependence is very weak.

The next Fig. 11 shows the dependence between durations of Sheath events and MC events (Fig. 11a) and Ejecta events (Fgi. 11b) adjoining them, but separately for two groups of events differing in the bulk velocity, $V < 450$ km/s (circles) and $V > 450$ km/s (black dots), in the beginning of MC and Ejecta following Sheath (the velocity was estimated for the first hourly point inside the events MC and Ejecta).

One can see in Fig. 11a that duration of Sheath adjoining MC event does not depend on the duration of MC itself for both groups of MC velocities. Similarly, duration of Sheath adjoining Ejecta does not depend on the duration of Ejecta event itself, independent of the bulk velocity of a leading part of the Ejecta event (Fig. 11b). In particular, duration of separate MC events can vary within wide limits between ~10 h and several days (50–60 h), but even in the case of relatively short duration of the very body of MC (about 10 h) the duration of Sheath region before it can vary in a very wide range, from 4 h to a day. A similar situation is also observed for Ejecta events.

Thus, durations of individual events vary for different types of the solar wind in a very wide range from several hours to several days. On the average, events HCS and Rare have in a year the shortest duration of ~5 h. The longest annual duration ~30 h belongs to Ejecta events. However, the scatter is large, and root mean square deviations are comparable in magnitude with the value of duration itself, therefore, it is impossible to speak about variations with the solar cycle. Averaged over the entire period, the MC duration is shorter than Ejecta duration and is equal to 85% of the latter. But when root mean square is ~50% of the duration ratio one can assume the equality of durations.

The duration of Sheath of Ejecta events is approximately 57% of Ejecta duration (i.e., a bit larger than a half). For MC events the duration of Sheath is approximately 46% (i.e., a bit smaller than a half). Taking into account the scatter which is higher for MC events, one can suppose that the duration of Sheath is identical for both types (MC and Ejecta) and equals ~50% of their duration. The mean ratio of Sheath durations for MC and Ejecta is 0.6 ± 0.4, i.e., duration of Sheath before MC is approximately twice shorter than before Ejecta (60% of Sheath duration of Ejects, but with a large scatter). A similar ratio is between the duration of Sheath region and duration of adjoining MC or Ejecta events (0.46 before MC and 0.61 before Ejecta). The duration of Sheath for MC and Ejecta does not depend on the duration of adjoining MC and Ejecta. Moreover, the value of velocity of the solar wind plasma inside adjoining MC and Ejecta events has no effect on the absence of any dependence of Sheath duration on the duration of adjoining MC and Ejecta.

3.3. Geoeffectiveness of the Solar Wind Events

In this paper we estimate geoeffectiveness of different types of the solar wind with respect to magnetic storms of moderate and strong intensity, i.e., having the value of D_{st} index at its minimum $D_{st} < -50$ nT. For each type of events the geoeffectiveness value was determined as a ratio of the number of events resulting in magnetic storms to the total number of events of the given type. It is assumed that a solar wind event results in a magnetic storm if the D_{st} minimum falls inside the event interval or follows it in no more than two hours.

In total, 798 moderate and strong magnetic storms with the intensity $D_{st} < -50$ nT were selected for the entire period of time. But only for 464 magnetic storms (i.e., for 58% of all magnetic storms) corresponding events were found in the solar wind. The sources of other 334 magnetic storms (i.e., of 42% of 798 storms) are uncertain, and this fact is mainly connected with the lack of data on plasma and interplanetary magnetic field which makes impossible to identify the solar wind type for given intervals.

Table 1 presents the total numbers of events of different types like CIR, Ejecta, and MC (with subtypes) (2nd column), the numbers of magnetic storms caused by these types of events (3rd column), and the values of total (over the full period 1976–2000) geoeffectiveness for corresponding event types (4th column).

It follows from Table 1 that 145 magnetic storms were caused by CIR events, which is 31.2% of 464 magnetic storms for which the solar wind types corresponding to them were identified; 96 magnetic storms (i.e., 20.7%) are caused by Sheath events (12 magnetic storms or 2.6% originated from Sheath region before MC, Sh_{MC}, and 84 magnetic storms or 18.1% were associated with Sheath region before Ejecta, Sh_E); 62 magnetic storms (13.4%) are connected with magnetic clouds MC (50 storms being by MC with Sheath (10.8%) and 12 by MC without Sheath (2.6%)); 161 magnetic storms (34.7%) are caused by Ejecta events (115 (24.8%) by Ejects with Sheath and 46 (9.9%) by Ejecta without Sheath). Thus, on average ~1/2 of magnetic storms are caused by Ejecta events, ~1/3 of magnetic storms are generated by CIR, and ~1/5 part of storms are due to Sheath region.

As is seen in Table 1, the total geoeffectiveness of CIR events is only 20.2%. The same geoeffectiveness value (20.4%) is typical for Ejecta events with Sheath, at the same time, geoeffectiveness of Ejecta events without Sheath region is only 8%. The largest geoeffectiveness is observed for MC events with Sheath and MC without Sheath, 63.3% and 54.5%, respectively. Approximately identical geoeffectiveness of 15% takes place for the Sheath region, no matter to which event type (MC or Ejecta) it is adjoining.

Notice that for the entire period from 1976 to 2000 approximately identical numbers of Ejecta with and without Sheath have been detected (563 and 575 events, respectively). However, magnetic storms are more frequently caused by events Ejecta with Sheath than by Ejecta without Sheath (115 events against 46 events). Thus, Ejecta events with Sheath are by a factor of 2.5 more geoeffective than Ejecta events without Sheath.

At the same time, the majority of MC events have Sheath region (79 events against 22), but this fact has small effect on their geoeffectiveness whose values are 63% and 54%, respectively. That is, the number of MC events with Sheath is four times larger than the number without Sheath, but the total geoeffectiveness of MC with Sheath is only by 8% higher than that for MC without Sheath.

Table 1. Geoeffectiveness of different types of the solar wind

Type of event	Events in total	Out of them with storm $D_{st} < -50$ nT	Geoeffectiveness of events
CIR	717	145	0.202
Sh_{MC}	79	12	0.152
Sh_E	543	84	0.155
MC with Sh	79	50	0.633
MC without Sh	22	12	0.545
Ejecta with Sh	543	115	0.212
Ejecta without Sh	585	46	0.078

Figure 12 shows year-to-year variations of (a) sunspot number and (b) geomagnetic storms with $D_{st} < -50$ nT, together with geoeffectiveness of the events: (*c*) CIR; (d) Sheath adjoining MC, Sh_{MC} (balck histiograms), and Ejecta, Sh_E (gray histograms); (e) MC having Sheath (black) and MC without Sheath (gray); and (f) Ejecta with Sheath (black) and Ejecta without Sheath (gray), respectively. The total (over the entire period) geoeffectiveness values for each type of events are presented on the right in panels (c–f).

Figure 2b presents the occurrence rate of magnetic storms (with minimum D_{st} index $D_{st} < -50$ nT) in the period 1976–2000. One can see a correlation with the solar activity (Fig. 12, panels (*a*) and (*b*)). Near the maximum of sunspot number the number of magnetic storms (~50–60) exceeds their number near the minimum (~8–15) by a factor of 4–5. Moreover, there is a tendency of peak separation into two parts, i.e., the maximum number of magnetic storms with intensity $D_{st} < -50$ nT is observed at the end of the growth phase and at the beginning of the declining phase of the solar cycle. A similar bifurcation of the peak for sunspots near the solar activity maximum is known as the Gnevyshev effect and is described in [42, 43]. Later, it has been demonstrated that the solar activity (in different manifestations: sunspots, CME, reversals of the polar field on the Sun) is characterized not by a single peak. A multiple structure of the maximum composed of 2–3 peaks is observed. This is possibly connected with restructuring of the magnetic field of the Sun in the polar regions, taking place near the maximum of solar activity [44]. It worthwhile to note more powerful and stable phenomena appear during the distrurbances during 2nd maximum, while the 1st maximum is characterized by numerous but weak events. The convenient position of the 2nd maximum (low latitudes) makes it more important for solar-terrestrial links [43].

As is seen in Fig. 12c, the annual geoeffectiveness of CIR events is variable in a wide range, from < 0.05–0.1 in the minimum of solar activity up to almost 0.4 in

different periods of different solar cycles. For example, one can suggest the existence in the 22nd cycle of activity of two peaks of CIR geoeffectiveness: the 1st peak near the solar activity maximum and the 2nd peak on the phase of solar activity decline. At the same time, a single peak of CIR geoeffectiveness is observed in the 21st and 23rd cycles, but at different periods: on the declining phase in the 21st cycle and on the phase of growth in the 23rd cycle of solar activity. One cannot see more clear and unambiguous dependence of geoeffectiveness of CIR events on the solar cycle.

Events of Sheath (see Fig. 12d) can accompany both MC (black histograms) and Ejecta (gray histograms) events. As is seen in Fig. 12d, the annual geoeffectiveness of Sheath is lower for Ejecta events than for MC events, and it does not exceed 0.4. At the same time, the Sheath geoeffectiveness for MC events is sometimes very high and can reach 1 (as was the case, for example, in 1990 when 3–4 MC events occurred, and all of them caused storms). On the other hand, if one excludes this year, the geoeffectiveness of Sheath events adjoining MC events does not exceed 0.5. Moreover, the total (for the time considered) geoeffectiveness of the Sheath region is virtually identical both for MC and for Ejecta events, being equal to 0.152 and 0.149, respectively. As one can see in Table 1, the total number of magnetic storms caused by Sheath regions is 96 (12 of them are associated with Sheath adjoining MC, and 84 storms are caused by Sheath adjoining Ejecta) out of all 642 (79 + 563) Sheath events accompanying both types MC and Ejecta. Then, the total geoeffectiveness of all Sheath events (accompanying MC and Ejecta) makes up 15%.

As is seen in Fig. 12e, annual values of geoeffectiveness for MC events of both subtypes (79 events of MC with Sheath and 22 events of MC without Sheath) vary in the range from 0.3 to 1, i.e., by a factor of 3. However, because of small statistics of events, the annual number of MC events without Sheath used to calculate geoeffectiveness is small and equals about 1–3 events, and only in 1978 as many as 6 events are recorded (out of them, 3 events resulted in magnetic storms, which corresponds to a geoeffectiveness of 0.5). Therefore, the annual geoeffectiveness of these MC events without Sheath, equal to 1, was estimated using 1–2 events of this type. For MC events with Sheath the annual number of events varied from 1 to 11. Therefore, the annual geoeffectiveness equal to 1 was estimated using 2–4 events of this type. That is, most MC events have a Sheath region (out of total MC number 101: 79 events have Sheath against 22 MC events without Sheath, or 78% against 22%), Because of small statistics of MC events one can only assume a tendency in variation of MC geoeffectiveness with the solar cycle, similar to the tendency for Ejecta events, magnetic clouds being a subtype of the latter (see below).

Figure 12f presents the annual distributions of geoeffectiveness for two subtypes of the Ejecta events: with Sheath (black histograms) and without Sheath (gray histograms). The annual geoeffectiveness of events Ejecta with Sheath varies in the solar cycle severalfold: from values of ~0.1 near the sunspot minimum up to values of about 0.4 on the declining phase near the maximum. Moreover, one can suggest bifurcation of the peak as for magnetic storms, i.e., existence of two peaks of Ejecta geoeffectiveness, on the phases of growth and decline of solar cycles. Notice that the annual number of these events associated with magnetic storms changes from 1 (near the minimum) up to 17 (near the maximum). A similar dependence is observed for Ejecta events without Sheath. But in this case the annual number of events causing storms is substantially lower and Varies in the range from 1 to 6 events.

Thus, the estimates show that the total geoeffectiveness for the entire time period from 1976 to 2000 for CIR events is 20.2% (only 145 events out of 717 have caused magnetic storms with intensity $D_{st} < -50$ nT). Geoeffectiveness of all Sheath (adjoining MC and Ejecta) for the full period 1976 to 2000 is 15.4% (only 96 Sheath events out of 622 are associated with magnetic storms). MC events, including both subtypes, with Sheath and without it, have the largest value of total geoeffectiveness, 61.3% (62 MC events out of 101 resulted in magnetic storms). The lowest total geoeffectiveness (14.2%) is demonstrated by Ejecta events, including both subtypes, with Sheath and without it (out of 1128 events only 161 caused magnetic storms). The total geoeffectiveness of events Ejecta with Sheath (21.2%) is approximately three times lower than that of events MC with Sheath (63.3%).

We emphasize that in total the events Ejecta and MC including all subtypes with Sheath and without it have the integral geoeffectiveness equal to 18.1% (out of 1128 + 101 = 1229 MC and Ejecta events 62 + 161 = 223 events caused magnetic storms). This means that geoeffectiveness 18.1% of all events ICME (including all subtypes Ejecta, MC, and Sheath) is close to geoeffectiveness 20.2% for CIR events. High geoeffectiveness of MC events that represent a subclass of events ICME is smeared when these events are joined with Ejecta due to their small number against the Ejecta background.

4. DISCUSSION OF RESULTS

4.1. Statistics of Events

It should be noted that, apparently, so far no systematic and comprehensive study of the occurrence rate of various type of the solar wind during several cycles of solar activity has been carried out. We have collected all published data on the numbers of different types of the solar wind and presented them together with our data in Fig. 13. A part of information was taken by us from tables presented in the papers, and some data on the event numbers sere taken from

the plots presented by authors in papers [15, 45, 47–57]. Depending on the method used, the number of events of one and the same type can differ strongly. In addition, the data of different authors belonging to one and the same time interval can be substantially divergent, since different authors have used both differing data sets and distinct selection criteria, which can be connected with a particular task of the paper's authors.

Figure 13 shows in the form of histograms (a) sunspot number, (b–f) number of solar wind events (without normalization) CIR, Ejecta, Sh_E, MC, and Sh_{MC}, respectively, that were taken by us from the catalog (partially, repeat of Fig. 2). The data of different authors [15, 45, 47–57] on the numbers of events of various types of the solar wind stream are superposed on the histograms in the form of points and lines. It is seen in Fig. 13 that more or less complete data of other authors covering almost the entire period 1976–2000 exist only for magnetic clouds MC, while for the other types of the solar wind the information is either unavailable or limited by very short intervals of time.

Magnetic clouds (MC) are a most frequently studied type of the solar wind. In Fig. 13e one can see a sufficiently good coincidence of the number of MC events selected by us with the data of satellites *Helios 1* and *Helios 2* for 1976–1980 period [45]. When identifying MC, authors of the latter paper used the basic property of MC events that distinguishes them from Ejecta: smooth variation of the magnetic field vector on time scales from a few hours to days [46]. A very good agreement is seen in Fig. 13e between our data and paper [45] in the period 1976–1980.

According to the data taken from another paper [47], the total number of MC events in the period from 1976 to 1993 is less by a factor of ~1.5 than we have found in the same period. Notice that in this paper MC events with complex magnetic field variations were excluded from consideration. As is seen in Fig. 13e the annual frequency of MC appearance turned out to be lower in comparison with our data.

The behavior of the occurrence rate of MC events during the 23rd cycle of solar activity (period 1996–2002) was studied in sufficient detail. As is seen in Fig. 13e, according to our data the peak of MC is observed on the growth phase of the 23rd cycle, which is confirmed also by the data of other authors (for example, [15, 48–51]). At the same time, the number of MC events according to our data drops down near 2000, but it grows by the results of other papers [15, 48, 50, 52, 53]. The observed distinction in the behavior of annual numbers of MC about 2000 is probably connected with incomplete statistics of MC events in 2000 due to the lack of data in the OMNI database.

In our data the majority of magnetic clouds (~70% of MC) have compression regions Sheath before them. In Fig. 13f it is seen that published data about Sheath events before MC are very scarce. The authors of paper [54] have found that in the period from 1998 to 2000 only ~48% of all MC had Sheath region. According to our data for the same three years the total fraction of events with Sheath before MC is higher and equals ~73%. The data on the number of Sheath before MC in 1997–2000 taken from paper [53] coincide with the data of [54].

Events ICME (Ejecta) for 1979–1988 were studied in papers [55, 56]. In [56], the authors used the data of *PVO (Pioneer Venus Orbiter)* for 1979–1988 and of *Helios-1* for the period 1974–1982. In order to investigate the connection of solar CME with interplanetary events ICME, the authors selected a certain configuration of the satellite location and the Earth–Sun line. It is this additional criterion that can explain the small number of Ejecta events observed for 10-year period in comparison with our data (see Fig. 13c).

In another paper [55] the authors determined the number of ICME events with a shock wave that foreruns the Sheath events. The number of such events Sheath before Ejecta is shown in Fig. 13d. Approximately a half of all ICME/Ejecta events in the period 1979–1988 had Sheath regions before them, both according to our data and according to the data of authors [55] (Figs. 13c and 13d).

In Fig. 13c one can see the different behavior of Ejecta (in our case) and ICME events of the authors of paper [48]. Notice that in [48], when identifying ICME events in the period 1996–2002, an additional criterion was used connected with the reduced intensity of galactic cosmic rays. According to our data, the number of Ejecta with Sheath does increase from the solar minimum to solar maximum of the 23rd cycle, but not so strongly, as in paper [48]. Such a discrepancy in behavior is, possibly, due to, firstly, differing method of identification of events in paper [48] (galactic cosmic ray decreases are caused mainly by variations of the IMF) and, secondly, small statistics of our events, especially in year 2000.

For the sake of clearness and because there are no other data we present in Figs. 13b, 13c, and 13d the numbers of CIR, Ejecta, and Sheath events from paper [57]. For their analysis the authors took separate small intervals inside the period 1997–2000, when geomagnetic disturbances were observed simultaneously with particle increases in the radiation belts, the *Mir* orbital station was irradiated, and the activity of induced current increased. Therefore, the statistics of events in paper [57] (shown in Figs. 13b, 13c, and 13d) is strongly underestimated and does not reproduce the real time behavior of these events.

Figure 13b presents the annual frequency of SIR and CIR events in the period 1979–1988 [55]. The CIR events were a subclass of SIR events, being distinguished only by recurrence or periodicity of events together with the solar rotation. Since CIR events identified by us include not only recurrent events, it is evident that closer coincidence should be observed with SIR events, as it is really seen in Fig. 13b. About observations of nonrecurrent high speed plasma

streams (at different phases of solar activity) it was reported in paper [58].

What is the fraction of magnetic clouds MC in the total number of ICME/Ejecta events, and how does it change with the solar cycle?

The results of our study show that the annual ratio of numbers of MC and Ejecta events averaged for the entire time period of 1976–2000 is equal to ~8%, but it varies between 5% and 22% for different years. One can suppose that the annual fraction of MC events several times higher on the phases of growth and decline of solar activity. The contribution of MC events to ICME was estimated for different solar cycles by the authors of papers [15, 48, 53, 59–61].

Most fully and comprehensively the MC fraction relative to ICME(Ejecta) has been studied for the 23rd solar cycle from 1995 to 2002 [15, 48, 59]. Over the entire time period the fraction of MC events in the total population of ICME events is equal to 25% and 15% according to the data of papers [48] and [59], respectively, which is comparable with our MC/Ejecta ratio (10% for the interval of 1996–2000), but is somewhat higher than the mean fraction MC/Ejecta ~8% obtained for 2.5 cycles of solar activity (see Fig. 7b). At the same time, for another period of 1978–1982 the fraction of MC was equal to only 14% of ICME events, which is close to our value of 8%. According to different estimates, the total fraction of MC in IMCE(Ejecta) changes in the wide limits from 14% up to 80% [62–70].

It should be noted that, according to the results of authors [15, 48, 59] the annual fraction of MC changes with the activity phase, the MC fraction being observed decreasing when one goes away from the solar minimum. Our results on variations of the MC fraction with the solar cycle are somewhat distinct from the conclusions made in papers [15, 48, 59]. The variation of the MC fraction with respect to Ejecta for the 21–23 activity cycles (according to our data) are shown in Fig. 7b. However, as one can see in Fig. 7b, the scatter of MC/Ejecta ratio is large, and, therefore, we can discuss only tendencies of variations. In order to answer unambiguously the question about variations of MC fraction with the activity cycle, one needs additional investigations with large statistics of MC events. We suggest that differing fractions of MC relative to Ejecta events obtained by different authors can be due to some distinctions both in criteria of event selection and in the data sets used by the authors. Spatial localization of satellites with respect to solar wind structures also can be involved.

4.2. Duration of Events

As a result of analysis of various types of the solar wind streams, using the OMNI database, we have demonstrated that mean duration of different types of events recorded in the time interval 1976–2000 varies in a wide range between ~5 h (HCS, Rare) and ~30 h (Ejecta). The scatter in duration of every type of events is also very large (see also [2]). The duration of Sheath region for both type of events MC and Ejecta is on average about 1/2 of the duration of the event itself.

How consistent are our results on duration of different type of solar wind streams with the data of other paper can be seen in Table 2, where our data on duration of different types of streams are given in the second column, and the data of other authors are presented in the third column.

One can see in Table 2 that the longest durations of 4.5 and 3 days were observed for events CIR and ICME/Ejecta at large distances from the Sun (5.3 AU) according to the data of *Voyager* mission [71]. The authors of [71] suggested that so long duration is often connected with a complex structure of events. In addition, duration of ICME (and of other types of the solar wind streams) depends on the trajectory of its propagation with respect to spacecraft.

It should also be noted that the duration of ICME events at 0.72 AU presented in paper [55] includes the duration of Sheath region, which often foreruns Ejecta (according to the data of these authors, it was observed in 65 out of 124 ICME). On the average, the Sheath region occupies approximately 16% of the duration of ICME/Ejecta according to the data of [55]. Our estimates made for a longer period of time give for the ratio of Sheath and Ejecta durations ~50% (see Fig. 9).

Different researchers estimated durations of solar wind events in limited periods of time. In [55] the data on duration of events CIR and ICME/Ejecta are presented for 11 years (the time period 1979–1988). They demonstrated that CIR duration was shorter near the solar activity minimum (1985–1988), which does not contradict our results (see Fig. 8c, where the variation of CIR duration within the limits of measurement scatter is shown). The ICME duration does not depend on the solar cycle [55], which is also not in contradiction with our results; though one can suppose that the maximum duration for Ejecta is observed near the maximum of the 21sr solar cycle (1980), but the amplitude of variation is within the scatter of measurements (see Fig. 8f). We emphasize once more that according to our data the scatter in duration of events is very large for every type of events (see vertical bars in Figs. 8 and 9), therefore, reliability of such conclusions is not sufficiently high.

Durations of magnetic clouds MC vary from a few hours to several days, which is consistent with the results of other papers [50, 52, 54, 73]. At the same time, one should remember that at so large distances as 2.6 AU from the Sun due to expansion of magnetic clouds their duration can increase up to 48–50 h, which is substantially longer than MC duration at 1 AU equal to ~24 h [45].

The values of 6–12 h for durations of Sh_E events presented in Table 2 have been obtained from a plot shown in Fig. 2 of paper [72] and are a rather rough

Table. 2. Durations of different types of the solar wind

Type of event	Mean duration $\langle dT \rangle$ h	Duration in other papers	References
HCS	4.98 ± 2.29		
CIR	20.17 ± 4.05	32.5 (7–122) h	[55]
		24–48 h	SIR [55]
		(4.5 ± 0.2) days	(5.3 AU) [71]
Sh_E	16.10 ± 3.71	16% $\langle dT_{ICME} \rangle$	[55]
		6–12 h	[72]
Sh_{MC}	9.48 ± 5.69		
Ejecta/ICME	29.12 ± 5.2	30.4 (6–86.4) h	[61]
		23.2 (18–30) h	[55]
		3.4 ± 0.4 days	(5.3 AU) [71]
		30.4 (6–86.4) h	[61]
MC	24.6 ± 11.67	A few hours – several days	[54]
		21.2 (3–55) h	[73]
		(10–46) h	[52]
		21.1 (2–30) h	[50]
Rare	4.49 ± 11.48	1–35 h	[74]

estimate of duration of the Sheath region before ICME/MC. First, we have used the ratio between the thickness of Sheath region and half-thickness of IMCE/MC region. This ratio for the IMCE/MC events analyzed by the authors of [72] varies between 0.4 and 0.9 (i.e., the thickness of Sheath region is 0.2–0.45 of the thickness of the event itself). Second, we assumed that the ratio between durations of Sheath region and adjoining events Ejecta and MC varies in a similar way, so that at a duration of ICME/MC event equal to ~1 day we obtain for Sheath duration values between 6 and 12 hours, which is lower than our estimates of Sheath duration (16 ± 3 h). It should be noted that measured durations of events, as well as the ratio between durations of Sheath region and adjoining events Ejecta and MC, depend on spatial geometry of a large-scale phenomenon of the solar wind and on the trajectory of a satellite crossing it. Therefore, for more reliable conclusions it is necessary to analyze multi-satellite observations together with model representations of the structure and geometry of these phenomena.

4.3. Geoeffectiveness of Events

The values of geoeffectiveness obtained by us for MC and Sheath before MC by averaging over the entire 25-years period are equal to 61.2% and 15%, respectively, and they can be compared with the values obtained by other authors. Many researchers studied MC in very limited periods of time, for example in the 23rd cycle of solar activity. In [54] it is demonstrated that about 80% of magnetic clouds MC can result in magnetic storms on the phase of growth and maximum of the 23rd solar cycle (1998–2000), while geoeffectiveness of the Sheath region is 9.6% [54], which is comparable with our values.

The importance of Sheath region adjoining MC and of some parts of MC proper (for example, the boundaries of a magnetic cloud) for excitation of magnetic storms was emphasized in papers [20, 21, 28, 75, 76]. The authors of [21] obtained for geoeffectiveness of Sheath region before MC the value (17.6%) that almost coincides with our estimates of the total geoeffectiveness (~15%). At the same time, geoeffectiveness of MC with Sheath is ~63% according to our data, which is substantially higher than 20.6% in paper [21]. From another paper [77] it follows that geoeffectiveness of magnetic clouds MC with respect to weak, moderate, and strong magnetic storms reaches 91%, which exceeds our results (~61%).

A detailed study of magnetic clouds (MC) and their geoeffectiveness during the 23rd solar cycle was performed in paper [53]. According to the data of these authors, geoeffectiveness of Sheath region is 22%, which is close to the value 15% obtained by us for the total geoeffectiveness of Sheath region in the period 1976–2000 and almost coincides with the value ~20% for geoeffectiveness of only 23rd cycle (see Fig. 9d). According to the same paper [53] geoeffectiveness of MC proper is higher by a factor of ~2 than geoeffectiveness of Sheath region and estimated as 48%, which is also close to our value of 61% for MC geoeffective-

ness in 1976–2000. Authors of [53] indicated that the type of magnetic cloud MC has a strong effect on the value of geoeffectiveness of a Sheath region. For example, for unipolar MC events, inside which the magnetic field has only the northern direction, geoeffectiveness of Sheath region reaches 67%. At the same time for a bipolar type of the MC structure (the field changes its direction from southward to northward or from northward to southward) geoeffectiveness of Sheath region is equal to 17% and 22%, respectively [53]. That is, a Sheath region causes a magnetic storm almost in 1/4 part of events (geoeffectiveness of Sheath is 25%) [53].

According to data of different authors, geoeffectiveness of magnetic clouds MC varies in the wide limits from 35% up to 70% [21, 48, 60, 78, 79]. Distinctions in geoeffectiveness of MC can be explained both by different methods of data analysis and by the direction of the process of analysis [17, 18].

On evidence of the data of authors [70, 80, 81] from 1/4 to 1/2 of all magnetic storms can be caused by the Sheath compression region of the solar wind preceding ICME/Ejecta events. According to our estimates for the period 1976–2000 about 31% of magnetic storms, for which drivers in the solar wind were identified, were caused by CIR events. This is also in agreement with the conclusions of the authors.

Investigations of CIR events for the period 1964–2003 have shown that ~34% of CIR events observed near the Earth are geoeffective and result in moderate and intense magnetic storms [19]. The obtained value of CIR geoeffectiveness is somewhat higher than our average value 20%.

According to paper [30], ICME/Ejecta events on average stronger manifest themselves in the D_{st} index than CIR events. For example, in the period 1996–2002 of the 23rd solar cycle the majority of CIR events causing magnetic storms occur near the minimum (1996) or the decline phase of solar activity. On the contrary, the number of ICME events and strength of the storms produced by them (minimum D_{st}) increases to the maximum of solar activity. However, according to our data for a similar time period 1996–2000 (Figs. 12c and 12f), the maximum number of geoeffective CIR events are observed near the maximum (1999), and geoeffective Ejecta events peak at the very maximum of the 23rd cycle (2000), which does not coincide with the results of authors of [30].

There is evidence in the literature that the occurrence rate of solar CME events has a peak near the solar maximum [82, 83], therefore, during the solar maximum ICME-driven storms dominate [11, 30, 79, 80, 84]. The frequency of appearance of CIR events (with 27-day periodicity) has a peak at the late declining phase of the solar cycle [85], therefore, storms on the declining phase are predominantly caused by CIR events [30, 58, 74, 80]. According to our data, indeed, geoeffective CIR events occur more frequently on the declining phase (21st and 22nd cycles), but they can also have a second peak near the maximum (for example, in the 22nd and 23rd cycles, Fig. 12c). As for geoeffective Ejecta events, they have bifurcated peaks near the maximum activity (one peak on every side from the maximum) (Fig. 12f).

Previously in paper [79] it was obtained that the fractions of magnetic storms from MC/Ejecta and CIR have two maximums (CIR in the maximum and minimum of the cycle) in the solar cycle and change in antiphase. This effect can be associated with two causes: (1) changing geoeffectiveness of MC/Ejecta and CIR events in the solar cycle (Fig. 12) and (2) changing relative numbers of MC/Ejecta and CIR events in the solar cycle (Fig. 7). Thus, the discovered effect [79] does not contradict the data of the present paper and can be associated with the relative number of events MC/Ejecta and CIR in the solar wind. However, to get an exact answer to the question about causes of existence of two maximums in every solar cycle for fractions of the magnetic storms from Ejecta and CIR events that change in antiphase requires additional investigations.

One can suppose that events ICME (MC) are the main source of moderate and intense magnetic storms, especially near the solar activity maximum. On the contrary, on the declining phase of the solar cycle the main source of geomagnetic activity is CIR events, i.e., compression regions formed by corotating high-speed streams streaming out coronal holes [60]. The average rate of appearance of intense magnetic storms near the solar maximum is higher by a factor 2–3 than it is observed on growing phases of the solar cycle near the minimum [60]. However, according to our data the occurrence rate of moderate and strong magnetic storms has two peaks near the maximum (on ascending and descending branches of the solar cycle). The trend of the frequency of geoeffective Ejecta events repeats the behavior of the frequency of magnetic storms of moderate and strong intensity (see Figs. 12b and 12f).

Thus, the data on geoeffectiveness of different types of large-scale streams of the solar wind obtained by us not only basically confirm the results of other authors obtained previously, but they substantially improve our knowledge embracing a long time period from 1976 to 2000.

CONCLUSIONS

In this paper we have determined the relative frequency of appearance of various types of the solar wind and their geoeffectiveness for moderate and strong magnetic storms with $D_{st} < -50$ nT, both integrally for the full time period and studying variations in the solar cycle over almost three solar cycle. This work was based on the catalog of large-scale types of the solar wind for the period of 1976–2000 (see ftp://ftp.iki.rssi.ru/pub/omni/) created by us on the basis of the OMNI database (http://omniweb.gsfc.

nasa.gov) [1] and described in detail in paper [2]. We have selected and analyzed 8 types of large-scale streams of the solar wind including subtypes (HCS, CIR, Sheath, Ejecta, MC, and Rare). All phenomena of Sheath type were divided in two subtypes: Sheath preceding Ejecta (Sh_E) and Sheath forerunning MC (Sh_{MC}).

The following conclusions are drawn as a result of our analysis.

1. Events HCS and Ejecta are the most frequent in the solar wind, events MC and Sheath before MC occur less frequently by an order of magnitude. Events CIR are recorded twice more rarely than HCS.

2. The occurrence rate of CIR events does not depend on the solar cycle, or this dependence is very weak. The largest number of HCS events is observed near the minimum of solar activity. Events Ejecta and MC (the total number of events, independent of existence/absence of a Sheath region) are more frequently observed on the phase of growth and near the maximum of solar activity; one can suppose that Sh_{MC} and Sh_E events have two peak: on the ascending and descending branches of the solar cycle.

3. Magnetic clouds MC are less frequent in the solar wind by an order of magnitude in comparison with Ejecta events. The fraction of MC (with respect to Ejecta events) increases near the phases of growth and decline of the solar activity, but it decreases by a factor of ~4 near the minimum and maximum of solar activity.

4. The majority of magnetic clouds (72%) have a Sheath region adjoining MC. But only about a half of Ejecta events have region Sheath (47%).

5. Mean annual fraction of MC with respect to CIR events is about 14%. The annual number of Ejecta events exceeds the annual number of CIR events by a factor of 1.63 ± 0.65.

6. The maximum fraction of Ejecta events (with respect to CIR) is observed on the growth phase of solar activity, and minimum is observed on the declining phase of the activity cycle, including its minimum.

7. During the full time from 1976 to 2000 the different type of the solar wind were observed: HCS for $6 \pm 4\%$, MC for $2 \pm 1\%$, Ejecta for $20 \pm 6\%$, Sheath before Ejecta for $8 \pm 4\%$, Sheath before MC for $0.8 \pm 0.7\%$, and CIR for $10 \pm 3\%$ of the total observation time. About 53% of the entire observation time fell on fast (Fast) type and slow (Slow) solar wind (21.5% and 31.5% of time, respectively).

The analysis of distribution of mean annual durations for different type of events has shown the following.

1. The mean duration of different types of events varies between ~5 h (HCS, Rare) and ~30 h (Ejecta) and is equal to: 5 ± 2 h for HCS events, 24 ± 11 h for MC, 29 ± 5 h for Ejecta, 16 ± 3 h for Sheath before Ejecta, 9 ± 5 h for Sheath before MC, and 20 ± 4 h for CIR.

2. When averaged for the entire period, the MC duration is shorter than Ejecta duration and is $\sim 85 \pm 50\%$ of the Ejecta duration.

3. Duration of Sheath of Ejecta and MC events is about a half of the duration of Ejecta and MC themselves. At the same time, the duration of Sheath region before MC is a half of the duration of Ejecta Sheath.

The results of analysis of the number of magnetic storms ($D_{st} < -50$ nT) are as follows.

1. The occurrence rate of magnetic storms is higher near the solar activity maximum by a factor of ~6 in comparison with the activity minimum.

2. Only for 58% of all magnetic storms their source in the solar wind have been classified, for 42% of magnetic storms no source was determined, basically, due to the lack of data. Out of 464 identified magnetic storms 31% were caused by CIR events, 21% were produced by Sheath region, ~13% and ~35% were generated by magnetic clouds MC and Ejecta events, respectively.

The analysis of geoeffectiveness of different type of the solar wind has shown the following concerning the magnetic storms.

1. MC events have the largest geoeffectiveness (54% for MC without Sheath, and 63% for MC with Sheath). The least geoeffectiveness is found for Ejecta events (8–14%). Geoeffectiveness of CIR events is ~20%. Geoeffectiveness of Ejecta events without Sheath (8%) is lower by a factor of 2.5 than that for Ejecta with Sheath (21%). The latter geoeffectiveness of Ejecta with Sheath (21%) is three times lower than for events MC with Sheath (63%).

2. The least value of geoeffectiveness for each type of events is observed near the minimum of solar activity. Two peaks of geoeffectiveness are possible for events Ejecta with Sheath: on the phases of growth and decline of solar activity.

Thus, for the first time a comparative study of occurrence rate and geoeffectiveness of all basic large-scale types of the solar wind was performed using a unified set of criteria for different parameters [2]. This was done for a long time interval embracing 2.5 solar cycles. The results presented are in general agreement with the results obtained by different methods on short time intervals. However, they give qualitatively new information, since they present for the first time a quantitative comparison of series of parameters for all types of the solar wind, including their variations with phases of the solar cycle.

ACKNOWLEDGMENTS

We appreciate the possibility of making use of the OMNI database. The data of OMNI were received from GSFC/SPDF OMIWeb on the website http://omniweb.gsfc.nasa.gov. The work is supported by the Russian Foundation for Basic Research, projects no. o4-02-16131 and no. 07-02-00042, and

by the Program OFN-15 "Plasma processes in the Solar system" and by RAS Presidium.

REFERENCES

1. King, J.H. and Papitashvili, N.E., Solar Wind Spatial Scales in and Comparisons of Hourly Wind and ACE Plasma and Magnetic Field Data, *J. Geophys. Res.*, 2004, vol. 110, no. A2, p. A02209. doi: 10.1029/2004JA010804.
2. Yermolaev, Yu.I., et al., Catalog of Large-Scale Solar Wind Phenomena during 1976–2000, *Kosm. Issled.*, 2009, vol. 47, no. 2, pp. 99–113. [*Cosmic Research*, pp. 81–94].
3. *Plazmennaya geliogeofizika, T. 1, T. 2* (Plasma Helio-Geophysics, vols. 1 and 2), Zelenyi, L.M, and Veselovsky, I.S., Eds., Moscow: Fizmatlit, 2008.
4. *Proc. of the Solar Wind 11/SOHO 16. "Connecting Sun and Heliosphere" Conference* (ESA SP-592). Held 12–17 June 2005, Whistler, Canada, Fleck, B., Zurbuchen, T.H., and Lacoste, H., Eds. Also Published on CDROM. ISBN 92-9092-903-0; ISSN 0379-6566 & 1609-042X (CD). Published by ESA Publications Division, ESTEC, Postbus 299, 2200 AG, Noordwijk, Netherlands, 2005.
5. Schwenn, R., Solar Wind Sources and Their Variations over the Solar Cycle, *Space Sci. Rev.,* 2006, vol. 124, p. 51. doi: 10.1007/s11214-006-9000-5.
6. Yermolaev, Y.I. and Yermolaev, M.Y., Comment on "Interplanetary Origin of Intense Geomagnetic Storms (D_{st} < –100 nT) during Solar Cycle 23" by W.D. Gonzalez et al., *Geophys. Res. Lett.*, 2008. doi: 10.1029/2007GL030281.
7. Dungey, J.W., Interplanetary Magnetic Field and the Auroral Zones, *Phys. Rev. Lett.*, 1961, vol. 6, p. 47.
8. Akasofu, S.I., Energy Coupling between the Solar-Wind and the Magnetosphere, *Space Sci. Rev.,* 1981, vol. 28, p. 121.
9. Russell, C.T. McPherron, R.L., and Burton, R.K., On the Cause of Geomagnetic Storms, *J. Geophys. Res.*, 1974, vol. 79, no. 7, p. 1105.
10. Perreault, P. and Akasofu, S.-I., A Study of Geomagnetic Storms, *Geophys. J. R. Astr. Soc.*, 1978, vol. 54, p. 547.
11. Gonzalez, W.D., Joselyn, J.A., et al., What Is a Geomagnetic Storm?, *J. Geophys. Res.*, 1994, vol. 99, p. 5771.
12. Gonzalez, W.D., Tsurutani, B.T., and de Gonzalez, A.L.C., Interplanetary Origin of Geomagnetic Storms, *Space Sci. Rev.*, 1999, vol. 88, nos. 3–4, p. 529. doi: 10.1023/A:1005160129098.
13. Bothmer, V. and Schwenn, R., Eruptive Prominences as Sources of Magnetic Clouds in the Solar Wind, *Space Sci. Rev.*, 1994, vol. 70, p. 215.
14. Lepping, R.P., Berdichevsky, D.B., et al., A Summary of WIND Magnetic Clouds for Years 1995–2003: Model-Fitted Parameters, Associated Errors and Classifications, *Ann. Geophys.*, 2006, vol. 24, p. 215.
15. Richardson, I.G. and Cane, H.V., The Fraction of Interplanetary Coronal Mass Ejections That Are Magnetic Clouds: Evidence for a Solar Cycle Variation, *Geophys. Res. Lett.*, 2004, vol. 31, p. L18804. doi: 10.1029/2004GL020958.
16. Pizzo, V.J., *Recurrent Magnetic Storms: Corotating Solar Wind Streams*, vol. 167 of *Geophysical Monograph Series*, Tsurutani, B., McPherron, R., Gonzalez, W., Lu, G., Sobral Jose, H.A., and Gopalswamy, N., Eds., Washington D.C.: AGU, 2006.
17. Yermolaev, Y.I., Yermolaev, M.Y., et al., Statistical Studies of Geomagnetic Storm Dependencies on Solar and Interplanetary Events: A Review, *Planet. Space Sci.*, 2005, vol. 53, p. 189.
18. Yermolaev, Yu.I. and Yermolaev, M.Yu., Statistic Study on the Geomagnetic Storm Effectiveness of Solar and Interplanetary Events, *Adv. Space Res.*, 2006, vol. 37, no. 6, p. 1175.
19. Alves, M.V., Echer, E., and Gonzalez, W.D., Geoeffectiveness of Corotating Interaction Regions as Measured by D_{st} Index, *J. Geophys. Res.*, 2006, vol. 111, A07S05. doi: 10.1029/2005JA011379.
20. Huttunen, K.E.J., Koskinen, H.E.J., and Schwenn, R., Variability of Magnetospheric Storms Driven by Different Solar Wind Perturbations, *J. Geophys. Res.*, 2002, vol. 107, no. A7, p. 1121. doi: 10.1029/2001JA900171.
21. Wu, C.-C. and Lepping, R.P., Effects of Magnetic Clouds on the Occurrence of Geomagnetic Storms: The First 4 Years of Wind, *J. Geophys. Res.*, 2002, vol. 107, no. A10, p. 1314. doi: 10.1029/2001JA000161.
22. Yermolaev, Yu.I., Yermolaev, M.Yu., and Lodkina, I.G., Comment on "A Statistical Comparison of Solar Wind Sources of Moderate and Intense Geomagnetic Storms at Solar Minimum and Maximum" by Zhang, J.-C., M.W. Liemohn, J.U. Kozyra, M.F. Thomsen, H.A. Elliott, and J.M. Weygand, *J. Geophys. Res.*, 2006. http://arXive.org/abs/physics/0603251.
23. Zhang, J.I., Richardson, G., et al., Solar and Interplanetary Sources of Major Geomagnetic Storms (D_{st} < –100 nT) during 1996–2005, *J. Geophys. Res.*, 2007, vol. 112, p. A10102. doi: 10.1029/2007JA012321.
24. Echer, E. Gonzalez, W.D., et al., Interplanetary Conditions Causing Intense Geomagnetic Storms (D_{st} < –100 nT) during Solar Cycle 23 (1996–2006), *J. Geophys. Res.*, 2008, vol. 113, p. A05221. doi: 10.1029/2007JA012744.
25. Yermolaev, Yu.I., Yermolaev, M.Yu., et al., Statistical Investigation of Heliospheric Conditions Resulting in Magnetic Storms, *Kosm. Issled.*, 2007, vol. 45, no. 1, pp. 3–11. [*Cosmic Research*, pp. 1–8].
26. Yermolaev, Yu.I. Yermolaev, M.Yu., et al., Statistical Investigation of Heliospheric Conditions Resulting in Magnetic Storms: 2,, *Kosm. Issled.,* 2007, vol. 45, no. 6, pp. 489–498. [*Cosmic Research*, pp. 461–470].
27. Huttunen, K.E.J. and Koskinen, H.E.J., Importance of Post-Shock Streams and Sheath Region as Drivers of Intense Magnetospheric Storms and High-Latitude Activity, *Ann. Geophys.*, 2004, vol. 22, p. 1729.
28. Vieira, L.E.A., Gonzalez, W.D., et al., Storm-Intensity Criteria for Several Classes of the Driving Interplanetary Structures, *Solar Physics*, 2004, vol. 223, p. 245.
29. Miyoshi, Y. and Kataoka, R., Ring Current Ions and Radiation Belt Electrons during Geomagnetic Storms Driven by Coronal Mass Ejections and Corotating Interaction Regions, *Geophys. Res. Lett.*, 2005, vol. 32, p. L21105. doi: 10.1029/2005GL024590.

30. Borovsky, J.E. and Denton, M.H., Differences between CME-Driven Storms and CIR-Driven Storms, *J. Geophys. Res.*, 2006, vol. 111, A07S08. doi: 10.1029/2005JA011447.

31. Denton, M.H., Borovsky, J.E., et al., Geomagnetic Storms Driven by ICME- and CIR-Dominated Solar Wind, *J. Geophys. Res.*, 2006, vol. 111, A07S07. doi: 10.1029/2005JA011436.

32. Guarnieri, F.L., Tsurutani, B.T., et al., ICME and CIR Storms with Particular Emphasis on HILDCAA Events, *ILWS Workshop, Goa, February 19–24, 2006.*

33. Plotnikov, I.Ya. and Barkova, E.S., Advances in Space Research Nonlinear Dependence of D_{st} and AE Indices on the Electric Field of Magnetic Clouds, *Adv. Space Res.*, 2007, vol. 40, p. 1858.

34. Yermolaev, Yu.I., Yermolaev, M.Yu., et al., Interplanetary Conditions for CIR-Induced and MC-Induced Geomagnetic Storms, *Bulg. J. Phys.*, 2007, vol. 34, p. 128.

35. Badruddin, P., Transient Perturbations and Their Effects in the Heliosphere, the Geo-Magnetosphere, and the Earth's Atmosphere: Space Weather Perspective, *J. Astrophys. Astr.*, 2006, vol. 27, p. 209.

36. Pulkkinen, T.I., Partamies, N., et al., Differences in Geomagnetic Storms Driven by Magnetic Clouds and ICME Sheath Regions, *Geophys. Res. Lett.*, 2007, vol. 34, L02105. doi: 10.1029/2006GL027775.

37. Yermolaev, Yu.I. and Yermolaev, M.Yu., Statistical Relationships between Solar, Interplanetary, and Geomagnetic Disturbances, 1976–2000: 3, *Kosm. Issled.*, 2003, vol. 41, no. 6, p. 574–584. [*Cosmic Research*, 539–549].

38. Farrugia, C.J., Matsui, H., et al., Survey of Intense Sun-Earth Connection Events (1995–2003), *Adv. Space Res.*, 2006, vol. 38, no. 3, p. 498.

39. Khabarova, O.V., Current Problems of Magnetic Storm Prediction and Possible Ways of Their Solving, *Sun and Geosphere*, 2007, vol. 2, no. 1, p. 32.

40. Gonzalez, W.D., and Echer, E., A Study on the Peak D_{st} and Peak Negative B_z Relationship during Intense Geomagnetic Storms, *Geophys. Res. Lett.*, 2005, vol. 32, L18103. doi: 10.1029/2005GL023486.

41. Yermolaev, Yu.I. and Yermolaev, M.Yu., Does Geomagnetic Storm Strength Depend on Solar Flare Importance?, *Kosm. Issled.*, 2009, vol. 47, no. 6, p. 495 [Cosmic Research, 460–465].

42. Gnevyshev, M.N., On the 11-Years Cycle of Solar Activity, *Sol. Phys.,* 1967, vol. 1, p. 107.

43. Gnevyshev, M.N., Essential Features of the 11 Year Solar Cycle, *Sol. Phys.,* 1977, vol. 51, p. 175.

44. Kane, R.P., Gnevyshev Peaks and Gaps for Coronal Mass Ejections of Different Widths Originating in Different Solar Position Angles, *Solar Phys.*, 2008, vol. 249, p. 369. doi: 10.1007/s11207-008-9185-9.

45. Bothmer, V. and Schwenn, R., The Structure and Origin of Magnetic Clouds in the Solar Wind, *Ann. Geophys.*, 1998, vol. 16, p. 1.

46. Burlaga, L.F, Magnetic Clouds, in *Physics of the Inner Heliosphere 2 – Particles, Waves and Turbulence*, Schwenn, R. and Marsch, E., Eds., New York: Springer, 1991, vol. 21, p. 1.

47. Bothmer, V. and Rust, M.D., in *Coronal Mass Ejections*, Crooker, N., Joselyn, J.A., and Feynman, J., Eds., vol. 99 of *Geophysical Monographs,* Washington D.C.: AGU, 1997, p. 137.

48. Cane, H.V. and Richardson, I.G., Interplanetary Coronal Mass Ejections in the Near-Earth Solar Wind during 1996–2002, *J. Geophys. Res.*, 2003, vol. 108, no. A4, p. 1156. doi: 10.1029/2002JA009817.

49. Mahrous, A., et al., Empirical Model of the Transit Time of Interplanetary Coronal Mass Ejections, *Solar System Research*, 2009, vol. 43, no. 2, p. 128.

50. Wu, C.-C., Lepping, R.P., and Gopalswamy, N., Relationships Among Magnetic Clouds, CMEs and Geomagnetic Storms, *Sol. Phys.*, 2006, vol. 239, p. 449. doi: 10.1007/s11207-006-0037-1.

51. Lepping, R.P. and Wu, C.-C., On the Variation of Interplanetary Magnetic Cloud Type through Solar Cycle 23: Wind Events, *J. Geophys. Res.*, 2007, vol. 112, A10103. doi: 10.1029/2006JA012140.

52. Lynch, B.J., et al., Internal Structure of Magnetic Clouds: Plasma and Composition, *J. Geophys. Res.*, 2003, vol. 108, no. A6. doi: 10.1029/2002JA009591.

53. Huttunen, K.E.J., Schwenn, R., et al., Properties and Geoeffectiveness of Magnetic Clouds in the Rising, Maximum and Early Declining Phases of Solar Cycle 23, *Ann. Geophys.,* 2005, vol. 23, p. 625.

54. Zhang, J.-C., Liemohn, M.W., et al., A Statistical Study of the Geoeffectiveness of Magnetic Clouds during High Solar Activity Years, *J. Geophys. Res.*, 2004, vol. 109, A09101. doi: 10.1029/2004JA010410.

55. Jian, L.K., Russell, C.T., et al., Stream Interactions and Interplanetary Coronal Mass Ejections at 0.72 AU, *Solar Phys.,* 2008, vol. 249, p. 85. doi: 10.1007/s11207-008-9161-4.

56. Lindsay, G.M., Luhmann, J.G., et al., Relationships between Coronal Mass Ejection Speeds from Coronagraph Images and Interplanetary Characteristics of the Associated Interplanetary Coronal Mass Ejections, *J. Geophys. Res.*, 1999, vol. 104, p. 12515.

57. Dmitriev, A.V., Crosby, N.B., and Chao, J.-K., Interplanetary Sources of Space Weather Disturbances in 1997 to 2000, *Space Weather*, 2005, vol. 3, S03001. doi: 10.1029/2004SW000104.

58. Bobrov, M.S., Non-Recurrent Geomagnetic Disturbances from Highspeed Streams, *Planet. Space Sci.*, 1983, vol. 31, p. 865.

59. Richardson, J.D. and Cane, H.V., A Survey of Interplanetary Coronal Mass Ejections in the Near-Earth Solar Wind during 1996 – 2005, *Proc. Solar Wind 11 – SOHO 16 "Connecting Sun and Heliosphere," Whistler, Canada, 12–17 June 2005*, ESA SP-592, September 2005.

60. Meloni, A., De Michelis, P., and Tozzi, R., Geomagnetic Storms, Dependence on Solar and Interplanetary Phenomena: A Review, *Mem. S. A. It.,* 2005, vol. 76, p. 882.

61. Liu, Y., Richardson, J.D., and Belcher, J.W., A Statistical Study of the Properties of Interplanetary Coronal Mass Ejections from 0.3 to 5.4 AU, *Planet. Space Sci.*, 2005, vol. 53, p. 3.

62. Richardson, I.G., Farrugia, C.J., and Cane, H.V., A Statistical Study of the Electron Temperature in Ejecta, *J. Geophys. Res.,* 1997, vol. 102, p. 4691.
63. Marubashi, K., Physics of Interplanetary Magnetic Flux Ropes: Towards Prediction of Magnetic Storms, *Adv. Space Res.*, 2000, vol. 26, p. 55.
64. Gosling, J.T, Coronal Mass Ejections and Magnetic Flux Ropes in Interplanetary Space, in *Physics of Magnetic Flux Ropes*, vol. 58 of *Geophysical Monographs*, Russell, C. T., Priest, E. R., and Lee, L.C., Eds., Washington D.C.: AGU, 1990, p. 343.
65. Mulligan, T., Russell, C.T., and Gosling, J.T., On Interplanetary Coronal Mass Ejection Identification at 1 AU, *Solar Wind Nine. AIP Conf. Proc.,* 1999, vol. 471, p. 693.
66. Cane, H.V., Richardson, I.G., and von Rosenvinge, T.T., Cosmic Ray Decreases: 1964–1994, *J. Geophys. Res.,* 1996, vol. 101, p. 21561.
67. Bothmer, V. and Schwenn, R., Signatures of Fast CMEs in Interplanetary Space, *Adv. Space Res.*, 1996, vol. 17, p. 319.
68. Cane, H.V., Richardson, I.G., and Wibberenz, G., Helios 1 and 2 Observations of Particle Decreases, Ejecta, and Magnetic Clouds, *J. Geophys. Res.,* 1997, vol. 102, p. 7075.
69. Henke, T., et al., Ionization State and Magnetic Topology of Coronal Mass Ejections, *J. Geophys. Res.*, 2001, vol. 106, p. 10957.
70. Owens, M.J., Cargill, P.J., et al., Characteristic Magnetic Field and Speed Properties of Interplanetary Coronal Mass Ejections and Their Sheath Regions, *J. Geophys. Res.*, 2005, vol. 110, A01105. doi: 10.1029/2004JA010814.
71. Jian, L.K. Russell, C.T., et al., Stream Interactions and Interplanetary Coronal Mass Ejections at 5.3 AU near the Solar Ecliptic Plane, *Solar Phys.*, 2008, vol. 250, no. 2, p. 375. doi: 10.1007/s11207-008-9204-x.
72. Russell, C.T. and Mulligan, T., The True Dimensions of Interplanetary Coronal Mass Ejections, *Adv. Space Res.*, 2002, vol. 29, p. 301.
73. Lepping, R.P., Wu, C.-C., et al., Forecasting the Intensity of Magnetic Storms Caused by NYS Type Interplanetary Magnetic Clouds, *Eos Trans. AGU*, 2005, vol. 86, no. (52). Fall Meet. Suppl. Abstract SH23A-0334.
74. Richardson, I.G., Dvornikov, V.M., et al., Bidirectional Particle streams at Cosmic Ray and Lower (~1 MeV) Energies and Their Association with Interplanetary Coronal Mass Ejections/Ejecta, *J. Geophys. Res.*, 2000, vol. 105, p. 12597.
75. Tsurutani, B.T., and Gonzalez, W.D, *The Interplanetary Causes of Magnetic Storms: A Review*, vol. 98 of *Geophysical Monographs*, Tsurutani, B. T., Ed., Washington D.C.: 2000, p. 77.
76. Gonzalez, W.D., Gonzalez, A.L.C., et al., Solar and Interplanetary Causes of Very Intense Geomagnetic Storms, *J. Atmos. Sol.-Terr. Phys.*, 2001, vol. 63, p. 403.
77. Wu, C.-C., Lepping, R.P., and Gopalswamy, N., Variations of Magnetic Clouds and CMEs with solar cycle, *Proc. ISCS 2003 Symposium "Solar Variability as an Input to the Earth's Environment," Slovakia, ESA,* 2003, vol. 1, p. 429.
78. *Vennerstro*en, S., Interplanetary Sources of Magnetic Storms: A Statistical Study, *J. Geophys. Res.*, 2001, vol. 106, p. 29175.
79. Yermolaev, Yu.I. and Yermolaev, M.Yu., Statistical Relationships between Solar, Interplanetary, and Geomagnetospheric Disturbances, 1976–2000, *Kosm. Issled.,* 2002, vol. 40, no. 1, p. 3–16. [*Cosmic Research*, pp. 1–14].
80. Richardson, I.G., Cliver, E.W., and Cane, H.V., Sources of Geomagnetic Storms for Solar Minimum and Maximum Conditions during 1972–2000, *Geophys. Res. Lett.*, 2001, vol. 28, p. 2569.
81. Tsurutani, B.T., Gonzalez, W.D., et al., Origin of Interplanetary Southward Magnetic Fields Responsible for Major Magnetic Storms near Solar Maximum (1978–1979), *J. Geophys. Res.*, 1988, vol. 93, p. 8519.
82. Webb, D.F., The Solar Cycle Variation of the Rates of CMEs and Related Activity, *Adv. Space Res.*, 1991, vol. 11, p. 37.
83. Yashiro, S., Gopalswamy, N., et al., A Catalog of White Light Coronal Mass Ejections Observed by the SOHO Spacecraft, *J. Geophys. Res.*, 2004, vol. 109, A07105. doi: 10. 1029/2003JA000504.
84. Richardson, I.G., Cane, H.V., and Cliver, E.W., Sources of Geomagnetic Activity during Nearly Three Solar Cycles (1972–2000), *J. Geophys. Res.*, 2002, vol. 107, no. A8, p. 1187. doi: 10.1029/2001JA000504.
85. Mursula, K. and Zeiger, B., The 13.5-Day Periodicity in the Sun, Solar Wind, and Geomagnetic Activity: The Last Three Solar Cycles, *J. Geophys. Res.*, 1996, vol. 101, p. 27077.